DOKUZ EYLÜL UNIVERSITY

GRADUATE SCHOOL OF NATURAL AND APPLIED SCIENCES

SYNTHESIS OF BIOACTIVE ORGANORUTHENIUM COMPLEXES

by

Egemen Orkun SADAN

August, 2022

İZMİR

SYNTHESIS OF BIOACTIVE ORGANORUTHENIUM COMPLEXES

A Thesis Submitted to the

Graduate School of Natural and Applied Sciences of Dokuz Eylül University

In Partial Fulfillment of the Requirements for the Degree of Master of Science

in Chemistry

by

Egemen Orkun SADAN

August, 2022

İZMİR

M.Sc THESIS EXAMINATION RESULT FORM

We have read the thesis entitled **"SYNTHESIS OF BIOACTIVE ORGANORUTHENIUM COMPLEXES"** completed by **EGEMEN ORKUN SADAN** under supervision of **PROF.DR. ELİF SUBAŞI** and we certify that in our opinion it is fully adequate, in scope and in quality, as a thesis for the degree of Master of Science.

Prof.Dr. Elif SUBAŞI

Supervisor

Prof. Dr. Funda Demirhan

(Jury Member)

Prof. Dr. Hülya Ayar KAYALI

(Jury Member)

Prof. Dr. Okan FISTIKOĞLU

Director

Graduate School of Natural and Applied Sciences

ACKNOWLEDGMENT

The research described in this thesis was done at Dokuz Eylül University, Faculty of Science, Department of Chemistry. The support and cooperation of many people in this study process have been precious for me. At least I owe those who helped me, and I want to offer my sincere thanks to them.

Firstly and most importantly, I want to thank my supervisor Prof. Dr. Elif SUBAŞI for her posed guidance and all-hearted support through my research work. And I would like to thank Mülkiye KAYMAZ and Utku ULUCAN for their kindly help.

Last, I want to thank especially my mother and my family for their moral support and love throughout my life. For these reasons, I have dedicated this work to them.

Egemen Orkun SADAN

SYNTHESIS OF BIOACTIVE ORGANORUTHENIUM COMPLEXES

ABSTRACT

Ruthenium complexes are attracting current interest as one variety of promising metal-base anticancer drugs because of their specific biological functions. This mainly because of their ability to form compounds with interesting electronic structures, uncommon co-ordination number, unusual stereochemistry, along with their broad spectrum of biologic areas, such as antiviral, antifungal, antibacterial, antioxidant activities, anticarcinogenic, antitumor, DNA binding abilities and insulin mimetic effects.

Herein antiproliferative activity, characterization and synthesis of "half-sandwich" organo-ruthenium(II) compounds [(η^6-*p*-cym)Ru(*N,S*-TSC)Cl]Cl (I, II and III), which TSC= 5-nitro-2-carboxyaldehyde-thiophen-*N*-methyl-thiosemicarbazone, (TSC^1); 2-acetyl-5-bromo-thiophen-*N*-methyl-thiosemicarbazone, (TSC^2) and 2-acetyl-5-bromo-thiophen-*N,N*-dimethyl-thiosemicarbazone, (TSC^3), were reported, respectively. The purified complexes were analyzed using many spectroscopic techniques like ^{1}H NMR spectroscopy, FT-IR, elemental analysis, single-crystal XRD, MALDI-TOF mass spectrometry and UV-Vis spectroscopy. These studies shows that TSCs demonstrate abilitiy to bind bidentate. This ligands have the property of binding via azomethine nitrogen atoms and thiocarbonyl sulphur metal atoms with all complexes (I, II, III). Crystalline forms of TSC^1 and TSC^2 were revealed by X-ray spectroscopy. These compounds crystallize with the P-1 space group in the triclinic crystal system. Biological potential studies were performed on TSC ligands and their ruthenium compounds (TSC1, TSC2 and TSC3) (I, II and III). Accordingly, studies were conducted on human primary ovary (A2780) and human metastatic ovary (OVCAR-3) cell lines. Our results highlight the impact that novel synthesized Ru(II) complexes can have superior biologic activity.

Keywords: Anticancer, antitumor activity, thiosemicarbazone, organoruthenium (II)-arene complexes

BİYOAKTİF ORGANORUTENYUM KOMPLEKSLERİNİN SENTEZİ

ÖZ

Rutenyum kompleksleri, spesifik biyolojik fonksiyonları nedeniyle umut verici metal bazlı antikanser ilaçların bir çeşidi olarak günümüzde ilgi çekmektedir. Bu esas olarak, farklı stereokimyasal kompleksler oluşturabilmesi, yaygın olmayan koordinasyon sayılarına sahip olması, ilginç elektronik yapılar ile birlikte geniş biyolojik aktivitelerinin olmasından kaynaklanmaktadır. Antiviral, antifungal, antibakteriyel, antitümör, antikanserojenik, antioksidan aktiviteler, insülin mimetik etkileri ve DNA bağlama yetenekleri bunlara örnek verilebilir.

Burada organo-rutenyum(II) yarı-sandviç komplekslerinin [(η^6-*p*-simen)Ru(*N,S*-L)Cl]Cl (I, II ve III), L= 5-nitro-2-karboksialdehit-tiyofen-*N*-metil-tiyosemikarbazon, (TSC^1); 2-asetil-5-bromo-tiyofen-*N*-metil-tiyosemikarbazon, (TSC^2) ve 2-asetil-5-bromo-tiyofen-*N,N*-dimetil-tiyosemikarbazon, (TSC^3) sentezi, karakterizasyonu ve antiproliferatif aktivitesi sırasıyla rapor edilmiştir. İzole edilmiş bileşikler, elementel analiz, FT-IR, ^{1}H NMR spektroskopisi, UV-Vis spektroskopisi, MALDI-TOF kütle spektrometrisi ve tek kristal XRD gibi spektroskopik teknikler kullanılarak analiz edildi. Bu çalışmalar, tiyosemikarbazon ligandlarının (TSC' ler), tüm komplekslerde (I, II ve III) metal iyonuna tiyokarbonil kükürt ve azometin azot atomları aracılığıyla koordine olan iki dişli bir ligand olarak bağlandığını göstermiştir. TSC^1 ve $TSC^{2'}$ nin X-ışını kristal yapıları, her iki bileşiğin de triklinik kristal sisteminde P-1 uzay grubu ile kristalleştiğini göstermektedir. Yeni sentezlenen TSC ligandlarının (TSC^1, TSC^2 ve TSC^3) ve bunlara karşılık gelen rutenyum komplekslerinin (I, II ve III) biyolojik potensiyeli, insan birincil yumurtalık (A2780) ve insan metastatik yumurtalık (OVCAR-3) hücre hatları üzerinde araştırıldı. Sonuçlarımız, yeni sentezlenmiş rutenyum(II) komplekslerinin potansiyel biyolojik aktiviteye sahip olabileceğinin etkisini vurgulamaktadır.

Anahtar kelimeler: Antikanser, antitümör aktivite, tiyosemikarbazon, organorutenyum(II)-aren kompleksleri

CONTENTS

Page

LIST OF FIGURES

Page

LIST OF TABLES

Page

CHAPTER ONE
INTRODUCTION

Since Werner's leading study, coordination chemistry has developed in a continued way. Currently, coordination compounds are included in an outlandish broad range of uses in catalysis, optical related applications, medicinal field and hydrometallurgical extraction. There have been important current interest in the chemistry of ruthenium, which is fundamentally because of its attractive photochemical, photophysical and redox properties. As all these properties are directed by the coordination environment around the central metal ion, complexation of ruthenium by ligands of selected types is of heavy importance (Das, Peng, Lee & Bhattacharya, 2004).

The electronic configuration of ruthenium have broadest range of oxidation states in their complexes. This happens due to its electron configuration is ($4d^7$ $5s^1$) makes this metal, together with osmium, special within all the elements. For instance oxidation state -2 in $[Ru(CO)_4]^{2-}$ to +8 in RuO_4 corresponding to d^0 to d^{10}. The coordination chemistry of ruthenium is directed by the oxidation states +2 and +3. Synthetic variability, high oxidation states, easy availability and sturdy qualities make ruthenium complexes perform adequately as catalysts. Ruthenium is kinetically inert, a 4d transition metal, demanding more extended reaction times and high temperatures for synthetic goals than nickel and copper, which are unstable 3d metals. Consequently, ruthenium complexes usually contain high stability, and ligand exchanging able to appear with a few rearrangements. Furthermore, this stability allows the ligands to be modified during coordinating with metal (Fanni, Murphy, Killeen & Vos, 2000).

Metal chelate Schiff base complexes have played a significant role in developing stereochemical models in the main group and transition metal coordination chemistry, mainly because of their structural variability, ease of preparation and stability (Shimakoshi, Goto, Tachi, Naruta & Hisaeda, 2001; Morris, Zhou, Stern & Nguyen, 2001; Cozzi, 2004; Jiménez & Belmar, 2005). For investigating their exciting and essential features, many numerous "Schiff bases" and complexes have been researched. Such as, photochromic properties and complexing ability towards some

toxic metals, catalytic activity in olefins hydrogenation and transfer of an amino group, and their ability to binding oxygen reversibly (Jones, Summerville & Basolo, 1979; Olive, G. H. & Olive, S., 1984; Sawodny & Riederer, 1977). The high affinity for the chelation of the Schiff bases against the transition metal ions is utilised in preparing their stable complexes. The developments in this field gained momentum only after the 1950s. Nowadays, the research field coping with "Schiff base metal complexes" is widely spread. It covers many broad and diverse topics, including the enormous fields of organometallic complexes and numerous properties of bioinorganic chemistry (Maurya, Pandey, Chaurasia & Martin, 2006; García-Raso, Fiol, Bádenas & Muñoz, 2001; El-Behery & El-Twigry, 2007).

Because of their distinct biological function, ruthenium complexes are drawing much attention as a promising metal based anticancer drug (Su et al, 2013). Which is a result of their ability to make complexes with unique stereochemistry, unusual coordination number, intriguing electronic structures, much as their broad range of biological activities, such as antifungal, anticarcinogenic, antiviral, antibacterial, antitumor, insulin-mimetic effects, antioxidant activities, DNA binding abilities (Ghosh et al, 2017).

Ruthenium piano-stool half-sandwich complexes are an up-and-coming antitumor and antimicrobial agent. These complexes stereochemistry presents a fine platform for making novel synthesised complexes by changing the coordinated arene, the labile group and chelated ligand. Also, both naturally available of Ru (II) and Ru (III) oxidation states are octahedral and slightly inert (Lapasam, Banothu, Addepally & Kollipara, 2020).

1.1 Schiff Bases

A Schiff base had created when aldehyde or ketone reacts with a primary amine under particular conditions. Structurally, Schiff bases are nitrogen analogues of ketone or aldehyde in which the carbonyl group have been replaced by an azomethine group or imine (Da Silva et al., 2011). The general Schiff base synthesis have shown in figure 1.1 and 1.2 (Siddiqui, Azad, Khan, A. R. & Khan, T ,2019).

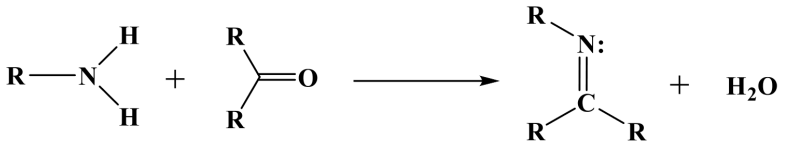

Figure 1.1 Schiff base reaction by condensation (Siddiqui, Azad, Khan, A. R. & Khan, T, 2019)

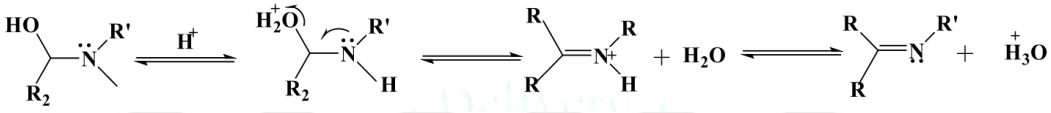

Figure 1.2 Reaction mechanism of Schiff base formation (Siddiqui, Azad, Khan, A. R. & Khan, T, 2019)

"Schiff bases" react with almost all lanthanides and transition metals, then form metal compounds (Sakthivel, Jeyasubramanian, Thangagiri & Raja, 2020). "Schiff bases" are shown to demonstrate a wide range of biological activities, including antibacterial, antiproliferative, anti-inflammatory, antifungal, antimalarial, antipyretic and antiviral properties (Przybylski, Huczyński, Pyta, Brzezinski & Bartl, 2009). Imine or azomethine groups are shown in many natural-derived, natural, and non-natural compounds (Figure 1.3) (Souza et al., 2007; Guo et al., 2007).

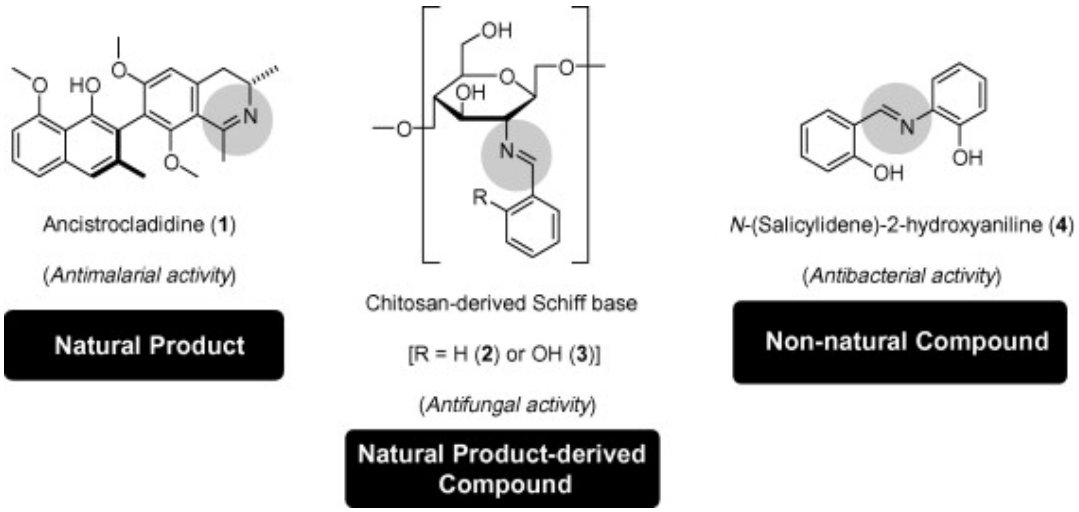

Figure 1.3 Examples of bioactive Schiff bases (Souza et al., 2007; Guo et al., 2007)

1.2 Ligands Types

TSCs are "Schiff bases" synthesized with condensation reaction between thiosemicarbazide and an "aldehyde" or a "ketone group". Thiosemicarbazones have two different categories which overall called as "bis and mono-thiosemicarbazones".

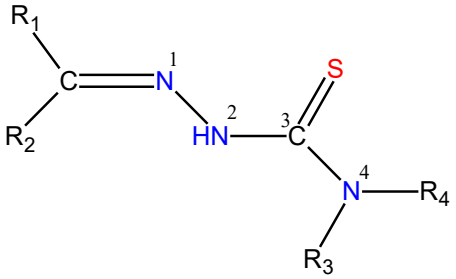

$$R_2CO + H_2N–NH–C(=S)– NH_2 \rightarrow R_2C=N–NH–C(=S)–NH_2$$

Figure 1.4 General structures of thiosemicarbazones

1.2.1 Mono-TSCs

The general mono-TSCs (Figure 1.4) have distinct substituents. Thiosemicarbazones are based upon aldehydes, which hydrogen atoms are substituent (R^2) at C2, meantime, R^1, can be heterocyclic group, an aryl or an alkyl. Likewise, substituents on N1 can be second aryl, an alkyl one or two hydrogen atoms. N1 can be piece of a "cyclic ring" as well. Various structures (II–V) are illustrated below (Figure 1.5). At Figure 1.6, Mono-TSCs relies on the ketones, therefore (R1) and (R2) groups at C2 can be the aryl or alkyl substituents (VI). Also, at category (VII), the ketone group is cyclic, hence C2 is a portion of structure (Lobana, Sharma, Bawa & Khanna, 2009).

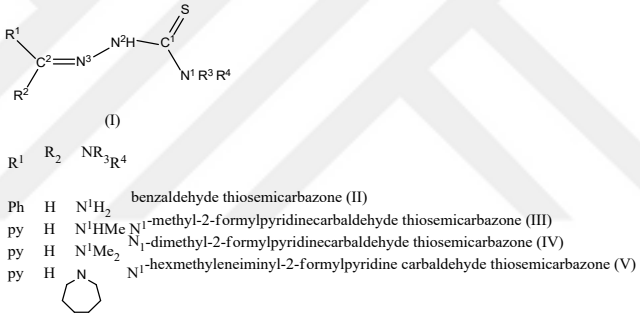

Figure 1.5 Structure of mono-thiosemicarbazones (II-V) (Lobana, Sharma, Bawa & Khanna, 2009)

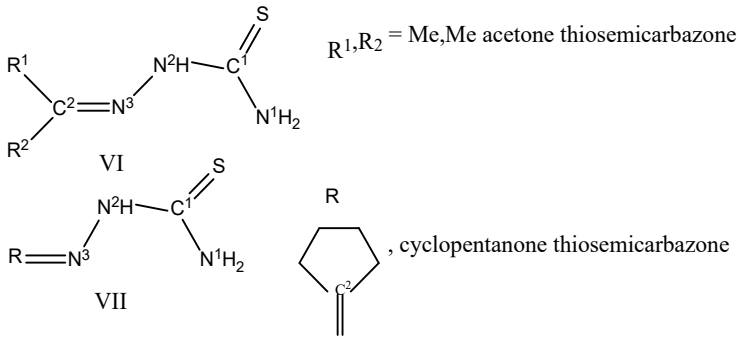

Figure 1.6 Structure of mono-thiosemicarbazones (VI-VII) (Lobana, Sharma, Bawa & Khanna, 2009)

1.2.2 Bis-TSCs

Bis-TSCs ring's and two arms joined and a C^2 - $C^{2'}$ bonded structures revealed (Figure 1.7).

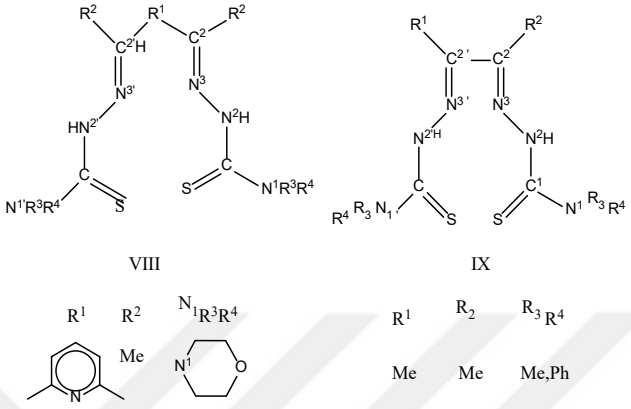

Figure 1.7 Structure of bis-thiosemicarbazones (VIII-IX) (Lobana, Sharma, Bawa & Khanna, 2009)

1.3 Bonding Modes TSCs

TSCs are as thione–thiol tautomers and can attach to a metal ion in the anionic or neutral structures. After the separation of H^+ from (-SH (Xb)) or (-N_2H (Xa)), the anionic structure is generated. Several bonding modes were observed for the TSCs in anionic or neutral forms (Figure 1.8).

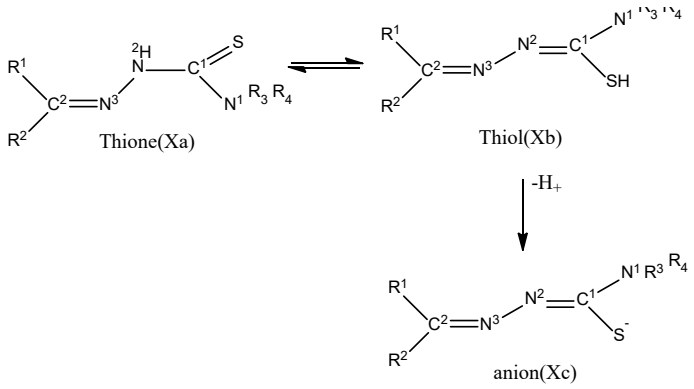

Figure 1.8 Thiol and thione form of thiosemicarbazones (Lobana, Sharma, Bawa & Khanna, 2009)

1.3.1 Neutral and Anionic Forms

In the "neutral form", molecule bonds formed only through S atoms, which they are showed as (XI-XVII) at (Figure 1.9). Nevertheless, if the substituent at C2 has a donor atom the other bonding modes are observed(XV, XVI and XVII) (X = O, N) (Lobana et al., 2006; Lobana, Khanna, Butcher, Hunter & Zeller, 2007; Lobana, Khanna & Butcher, 2007; Lobana, Kumari & Butcher, 2008; Jouad, Riou, Allain, Khan & Bouet, 2001; Lhuachan, Siripaisarnpipat, & Chaichit, 2003; Bermejo et al, 1999; Gómez-Saiz et al., 2003; Labisbal et al., 2003).

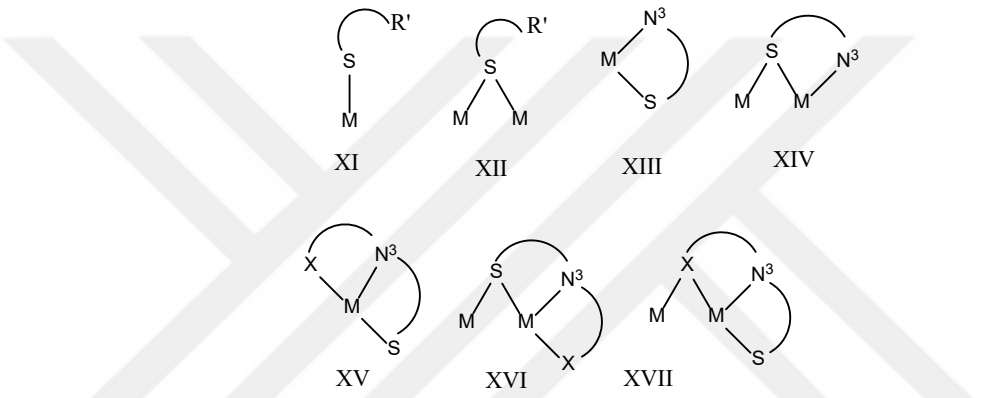

Figure 1.9 Bonding modes in neutral form (Lobana, Sharma, Bawa & Khanna, 2009)

Table 1.1 Bonding modes of TSCs (Lobana, Sharma, Bawa & Khanna, 2009)

Complexes	***Binding Modes***
XI	η^1-S
XII	μ_2-S
XIII	η^2-N^3, S-chelation
XIV	η^3-N^3, S-chelation and S-bridging
XV	η^3-X, N^3, S-chelation
XVI	η^4-X, N^3, S-chelation and S-bridging
XVII	η^4-X, N^3, S-chelation and X-bridging
XVIII	η^2-N^2, S
XIX	N^2, S-bridging and S-bridging modes

For “anionic form”, η^2-N2, S and N2, S-bridging, and S-bridging modes are identified (Figure 1.10) (Lobana, Bawa, Butcher, Liaw & Liu, 2006; Ashfield, Cowley, Dilworth & Donnelly, 2004). A rare example of pentacoordination of TSC has also been explained (Pal, Basuli, Mak & Bhattacharya, 2001).

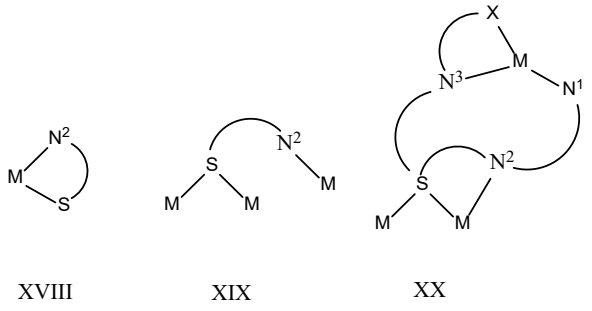

XVIII XIX XX

Figure 1.10 Bonding modes in anionic form (Lobana, Sharma, Bawa & Khanna, 2009)

1.3.2 Bonding Modes Bis-TSCs

Bis-TSCs can form complexes with both arms through binding to both anionic and neutral structures at (Figure 1.11) (XXI, XXII) (Gil, Bermejo, Castineiras, Beraldo, & West, 2000; Pedrido et al., 2005; Casas, et al., 2003).

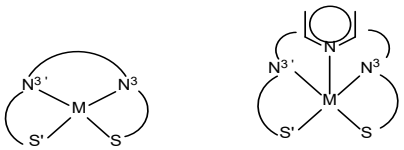

XXI XXII

Figure 1.11 Bonding modes of bis-thiosemicarbazones (Lobana, Sharma, Bawa & Khanna, 2009)

1.4 Properties of Metal Complexes and Metal-Based Compounds

Transition metals are “d” block elements, and they are in groups III–XII of the periodic table (Pattan, Pawar, Vetal, Gharate & Bhawar, 2012). They maintain individual features; which includes:

Charge variation: Metal ions occurs as positively charged in an aqueous solution. The charge can be modified to make a cationic, anionic or neutral state depending on

the existing coordination compounds (Haas & Franz, 2009). In addition, they may attach to negatively charged biological molecules by making positive charged ions in the aqueous solution (Frezza et al., 2010).

Structure and bonding: Metal complexes have a broad range of coordination geometries that provide them with distinctive shapes. Coordination site, bond length and bond angle vary depending on its oxidation state and metal (Haas & Franz, 2009). Structurally modified metal-based complexes have unique molecular species. These give a broad spectrum of coordination numbers, shapes and kinetic properties that organic molecules cannot duplicate (Frezza et al., 2010; Yan, Melchart, Habtemariam & Sadler, 2005; Salga, Ali, Abdulla & Abdelwahab, 2012).

Metal–ligand interaction: Metal-ligand interactions generally cause the formation of compounds which are distinctive from their individual metals or ligands. Ligand exchange reactions are affected by metal-ligand interactions' kinetic and thermodynamic properties (Haas & Franz, 2009). Supporting this reaction as metal shows a broad range of benefits to the metals to interact and coordinate with biological molecules (Frezza et al., 2010)

Lewis acid properties: Most metal ions are described as having high electron affinity, which can quickly polarize groups that are coordinated, therefore easing their hydrolysis (Frezza et al., 2010; Haas & Franz, 2009).

Partially filled d shell: Number of electrons in the d or f shell (for lanthanides) affects transition metal complexes' magnetic and electronic properties (Haas & Franz, 2009).

Redox activity: Many transition metals tend to experience reduction and oxidation reactions (Haas & Franz, 2009). The oxidation form of these metals is a critical concern in the design of the coordination molecules. In biochemical redox catalysis, metal ions often activate coordinated substrates and participate in redox active sites for charge cumulation.

Metal based molecules and metal complexes have ligands in a three-dimensional configuration, which allows them to functionalize groups that may be shaped to specified molecular targets (Frezza et al., 2010).

(η^6-Arene) Ru compounds that have piano-stool structures are the furthest researched ones. Their applications in catalysis, supramolecular assemblies, molecular devices, and antiviral, antibiotic, and anticancer activities have been discovered. These complexes have a pseudooctahedral shape at the Ru(II) ion, (η^6-arene) ligand has three coordinating sites with three other ligands (Figure 1.12) (Therrien, 2009).

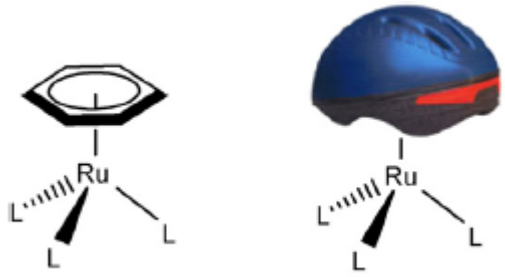

Figure 1.12 3 remaining coordination sites for ligands L (Therrien, 2009)

The occurrence of the aromatic π ligand preserve central metal, hindering quick oxidation to Ru(III). Furthermore, as spectator ligands, (η^6-arene)s are relatively inert towards substitution reactions. The arene moiety can have functionalised substituents and by this way the properties of the arene-Ru complexes can be. A broad range of ligands with N-, O-, S- or P-donor atoms can be placed at the remaining three coordination sites opposite to (η^6-arene). These complexes are dicationic, mono- or neutral, and frequently these ligands are labile (Therrien, 2009). Ligand exchange inside solution is essential at "self-assemblies" (Fujita, Tominaga, Hori & Therrien, 2005) and catalytic processes (Bennett, 1997).

1.5 Synthetic Methods

With research and improvement by other groups (Winkhaus & Singer 1967; Zelonka & Baird, 1972; Bennett et al., 1982), the most generally used synthesising of the (η^6-arene) Ru complexes are of $RuCl_3 \cdot nH_2O$ with a cyclohexadiene in an mixed EtOH-H_2O solution (**A**)(figure 1.13). Chloro-bridged dimers are mostly air stable products and ability form a bond with broad range of ligands, utilizing cleavage of the

"chloro-bridged" to make superior yield mononuclear half-sandwich complexes. (Robertson & Stephenson, 1976):

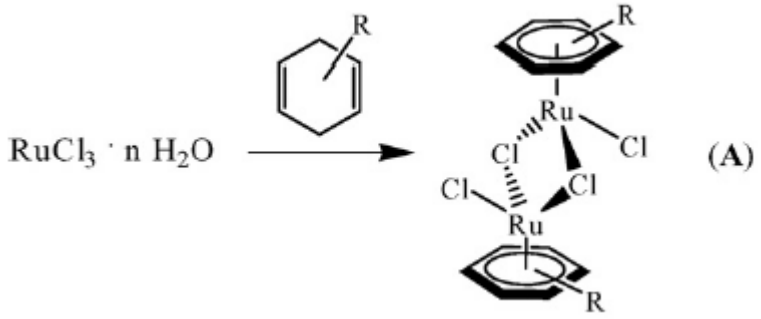

Figure 1.13 Arene ruthenium complex (Therrien, 2009)

Generating (η^6-arene) Ru compounds includes the exchange of the π-ligand at high temperatures in a second path (**B**) (Bennett & Smith, 1974) (Figure 1.14). This operation were considerably researched (Muetterties, Bleeke & Sievert, 1979). The arene exchange occurs concerted or in a stepwise way with the incoming arene. Before or during the insertion of the novel arene ligand, it is persistently released as η^6 to η^4 to η^2 states, which they released from coordination sphere. Furthermore, hexamethylbenzene ruthenium derivative is one of the best stable Ru arene parts, which they have electron rich properties. These ligands have electron acceptor groups that are modified with ease:

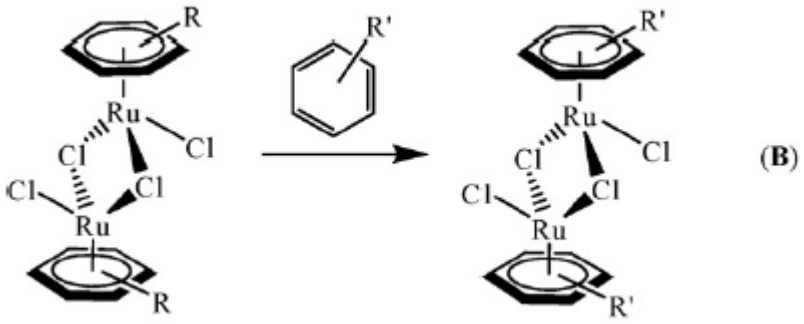

Figure 1.14 Hexamethylbenzene ruthenium complex (Therrien, 2009)

Two different methods were used to prepare half-sandwich (η^6-arene) Ru complexes. The first reaction indicates an intramolecular "Michael addition reaction" between the η^6-arene ligand and its attached arm (**C**) (Figure 1.15), meanwhile second

one utilises with Ru complexes that coordinated with biaryl ligand (**D**) (Figure 1.16) (Ghebreyessus & Nelson, 2000; Geldbach, Pregosin, Albinati & Rominger, 2001):

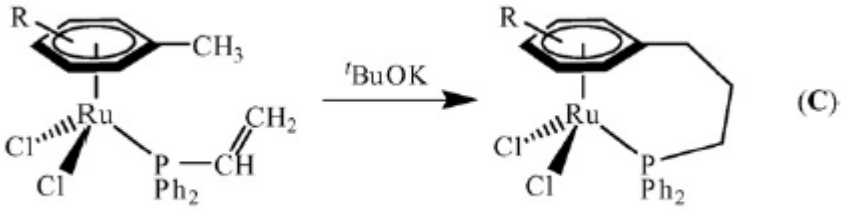

Figure 1.15 "Michael addition reaction" between the η^6-arene ligand and its attached arm (Therrien, 2009)

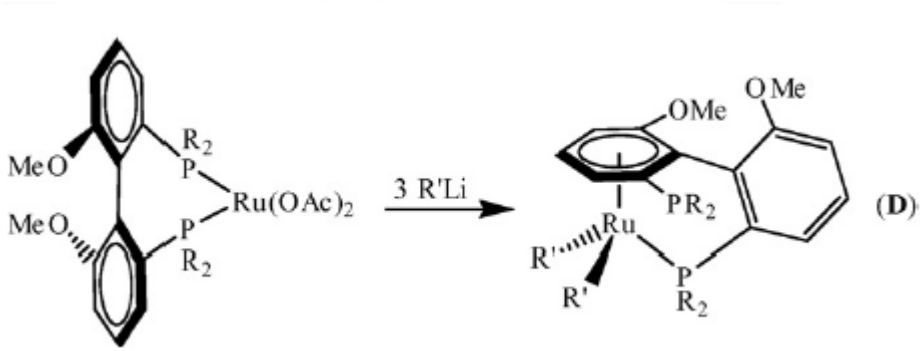

Figure 1.16 Ru complexes that coordinated with biaryl ligand (Therrien, 2009)

Various synthesis methods associated with fairly attainable materials supports chemistry of (η^6-arene) Ru complexes.

1.6 Ru(II) Compounds Cellular Uptake

In selective and efficacious cancer therapy, the uptake of Ru compounds by cancer or other cells is essential. The cell membrane possesses various proteins and lipids, which regulate what substances enter the cells. Ru(II) compounds enter cells via numerous mechanisms, like active transport, passive diffusion, and endocytosis (Gill & Thomas, 2012). Nevertheless, it is reported that most Ru compounds penetrate cells with endocytosis (Figure 1.17) (Zhou et al., 2016; Liang, Wei, Evans & Duan, 2014;

Zeng et al., 2017). ICP-MS, confocal laser scanning fluorescence microscopy, transmission electron microscopy and flow cytometry are frequently used to define the "intracellular accumulation" of Ru complexes (Puckett & Barton, 2007).

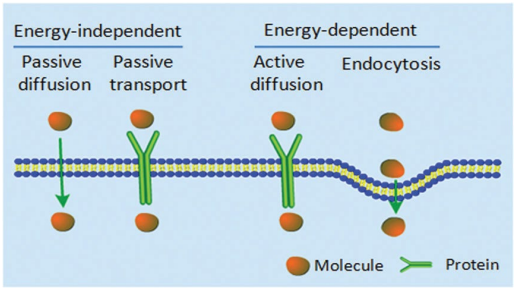

Figure 1.17 Drugs cellular uptakes (Zeng et al., 2017)

Cellular uptake and cellular localization can modulate with changed ligands and hydrophobicity. The "intracellular distribution" of Ru compounds in cells was explained as (a) the size and structure of ligand; (b) lipophilicity; (c) ionic charge (Puckett, Ernst & Barton, 2010; Zeng et al., 2017).

1.7 Ru(II) Compounds Potential Targets

There are various compounds with unique forms and proper functions, particularly proteins and DNA, which plays essential parts in defining "cellular activity" (Komor & Barton, 2013; Casini et al., 2007). Understanding the way of interaction between the Ru complex and its targets it is important for studying the anticancer mechanism and picking the most efficient compounds for effective and selective therapy.

1.7.1 Targeting DNA

Cancer cell proliferation is controlled by DNA which have a high proliferation rate and many Ru complexes have high selectivity as targeting DNA reported (Zhao et al., 2009; Zeng, Xiao, Liu & Tan, 2012; Aird et al., 2002; Pascu, Hotze, Sanchez-Cano, Kariuki & Hannon, 2007; Wu et al.,2013). The metal atoms which positive charged in these compounds may act like "electron acceptors", for negatively charged DNA

nucleophiles by the hydrolysis of ligands. Also, Ru compounds can attach to DNA through interaction with aromatic ligands. The noncovalent and covalent binding are the major binding modes between Ru and DNA compounds. The "non-covalent binding" of Ruthenium compounds are generally reversible and take places as intercalation, groove and electrostatic binding. Intercalation happens when planar arene complex are took place between neighbouring base pairs in double helix of DNA. The covalent binding is irreversible. For instance, Ru [(Ŋ^6-arene)Ru(en)Cl][PF_6] (en = ethylenediamine, arene = biphenyl) compounds able to bind covalent binding. The covalent binding mode between Ruthenium and DNA deforms the DNA backbone and weaken DNA transcription and replication (Turro, 2011).

Chao et al. synthesized novel cyclo-ruthenated complex. This compound had IC_{50} values lower than cisplatin (Figure 1.18) (Huang et al., 2014; Zeng et al., 2017).

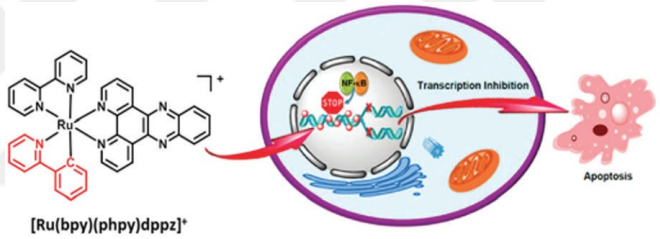

Figure 1.18 The anticancer effect of $[Ru(bpy)(phpy)dppz]^+$ (Zeng et al., 2017)

1.7.2 Proteins as Targets

Specific proteins might be targets for Ru compounds, particularly protein kinases (Zhang, Carroll & Meggers, 2004; Meggers, 2009; Aman et al., 2017; Babak et al., 2015). Particular enzymes play vital functions at "metabolic pathways" which were related with "cancer cell proliferation", "intercellular uptake" and "cell death" (Kilpin & Dyson, 2013). Ruthenium (II) compounds has strength to inhibition of protein kinases because of their facile, physicochemical properties and three dimensional structure. By modifying the ligands, the targeting ability and various functions of Ru compounds can be arranged (Blanck et al., 2012; Meggers, 2007). In the earlier work

Ru(II) polypyridyl complexes synthesized to act as (AChE) inhibitors (Dwyer, Gyarfas, Rogers & Koch, 1952).

1.8 Cell Death Process

Cell death can be present through many mechanisms (Figure 1.19) (Tan, Lu, Ji & Mao, 2014). Apoptosis is primarily induced, which are intrinsic and extrinsic pathways (Tan, Lu, Ji & Mao, 2014). The intrinsic pathway, called as the mitochondria mediated pathway, is triggered by endoplasmic reticulum (ER) stress, oxidative stress and DNA damage (Zheng, Wu, Wang, Tan & Mei, 2017). These condition can generate the mitochondrial discharge of "cytochrome c", which can trigger the apoptosis (Qian et al., 2013; Wang et al., 2014; Cao, Zheng & Chen, 2015; Liu, Y., Chen, Liu, J., & Wong, 2013). Generally, "non-apoptotic cell death" happens with ER stress or necrosis (Tan, Lu, Ji & Mao, 2014).

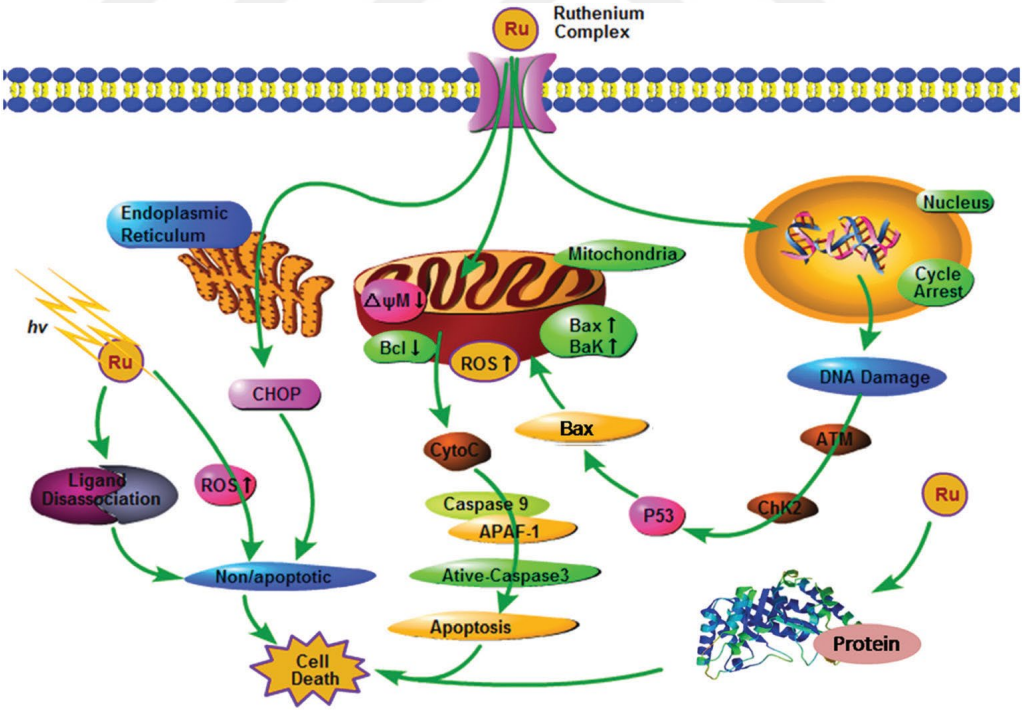

Figure 1.19 Overall presentation mechanism of action of Ru complexes that used as anticancer drug (Zeng et al., 2017)

CHAPTER TWO
MATERIAL AND METHODS

2.1 Materials

All reagents were used as received. $RuCl_3 \cdot nH_2O$, *N*-methyl/*N,N* dimethyl-3-thiosemicarbazide, 2-acetyl-5-bromo-thiophen, α-phellandrene, 5-nitro-2 carboxyaldehydethiophen, and other chemicals were purchased from SigmaAldrich. The reactions were executed using standard Schlenk line techniques under an inert argon atmosphere, and every glassware were dried in oven (120 °C) at night. Dry solvents were bought from SigmaAldrich and stored under inert gas. $[\{(\eta^6\text{-p-cym})RuCl\}_2(\mu\text{-}Cl)_2]$ was synthesized according to literature procedures (Bennett & Smith, 1974).

2.2 Instruments

LECOCHNS-O-9320 was performed for elemental analyses, Varian 1000 FT spectrophotometer (KBr pellets) was used for FT-IR spectra, ^1H NMR data were obtained in DMSO on High-Performance Digital FT NMR (400 MHz) and chemical shifts were internally referenced to tetramethylsilane (TMS). The UV-VIS spectra were recorded by Thermo-Scientific Evolution 600 Instrument. Excitation-emission spectral characteristics of the complexes were measured in steady-state mode of a fluorescence spectrometer (Edinburgh Instruments of FLS920). Mass analyses were recorded on a Bruker MALDI–TOF (Matrix-Assisted Laser Desorption/Ionization Time-Of-Flight) spectrometer using 1, 8, 9- trihydroxyanthracene as a matrix for the ligands and their ruthenium complexes. Conductance measurements were recorded on a Systronics automatic precision bridge 304 conductivity meter.

2.3 Synthesis of the TSC Ligands

The synthesis of ligands TSC^1, TSC^2 and TSC^3 were executed as following literature method (Yaman, Şen, Karagöz, & Subaşı, 2017).The aldehyde (1 mole equivalent) was dissolved in hot absolute ethanol solution (50 mL) and ambient conditions were created by a few drops of concentrated sulfuric acid. Same amount of TSC (1 mol eq.) was added to the reaction medium. Then the solution mixed in reflux condition at high temperature (4 hours). After the reaction was terminated, solution was cooled to ambient temperature the synthesized TSCs acquired as a precipitate. Solids obtained after filtration were washed with ethanol several times and dried under vacuum.

2.3.1 Synthesis of 5-Nitro-2-carboxyaldehydethiophen-N-methylthiosemicarbazone, TSC^1

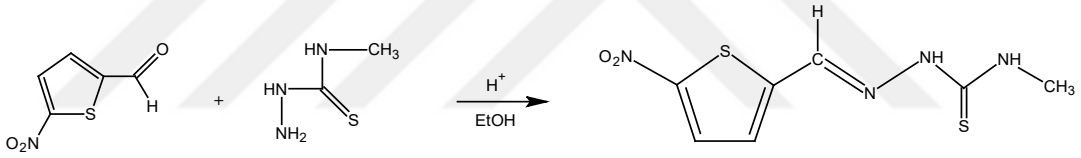

Figure 2.1 TSC^1 Synthesis

5-nitro-2-thiophene carboxyaldehyde (1 mol) and 4-methyl-3- thiosemicarbazide (1 mol) was mixed with absolute ethanol solvent (50 mL). The mixture heated up until it dissolved completely. Then concentrated sulfuric acid were added as a few drops. The solution mixed under reflux at high temperature (4 hours). After waited for cool down of solution, the TSC^1 ligand acquired as a precipitate. Finally, the solution was filtrated, washed with ethanol. Then the dried in vacuo (Figure 2.1). Single crystals were obtained by ethanol solution of TSC^1.

Orange powder, yield: 90%. $C_7H_8N_4S_2O_2$: Calc. %C: 34.42; H: 3.30; N: 22.93; O: 13.10; S: 26.25. Found: %C: 34.82; H: 3.17; N: 22.66; O: 13.87; S: 25.85. FTIR (KBr pellet), υ/cm^{-1}: 3339 (s), 3142 (s), 3105 (s) ($\nu(N_{(1)}H+N_{(2)}H)_{sym}$), 1564 (s), 1537 (s) ν(C=N), 1037 (s) ν(N-N), 908 (s) ν(C=S), 731 (s), 694 (s) (thiophen ring stretchings). ^{1}H NMR (400 MHz, DMSO-d_6) δ 11.81 (s, 1H, **H**C=N), 8.51 (s, 1H, $N_{(2)}$**H**), 8.18 (s,

1H, N(1)**H**), 8.05 (d, J = 4.26, 1H, thiophen ring protons); 7.49 (d, J = 4.24, 1H, thiophen ring protons), 2.99 (d, J = 4.40, 3H, NH**C**$\mathbf{H_3}$). MALDI-TOF MS: m/z= 244 [M^+].

2.3.2 Synthesis of 2-Acetyl-5-bromo-thiophen-N-methyl-thiosemicarbazone, TSC²

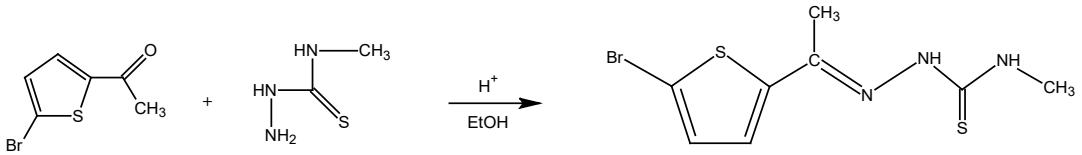

Figure 2.2 TSC^2 Synthesis

2-Acetyl-5-bromothiophene (1 mol equiv) and 4-methyl-3-thiosemicarbazide (1 mol eq.) was mixed with absolute ethanol solvent (50 mL). The mixture heated up until it dissolved completely. Then concentrated sulfuric acid were added as a few drops. The solution mixed under reflux at high temperature (4 hours). After waited for cool down of solution, the TSC^2 ligand acquired as a precipitate. Finally, the solution was filtrated, washed with ethanol. Then the dried in vacuo (Figure 2.2).

Yellow powder, yield: 85%. $C_8H_{10}N_3S_2Br$: Calc. %C: 32.88; H, 3.45; N, 14.38; S, 21.95. Found: %C: 32.23; H, 3.12; N, 14.22; S, 21.44. FTIR (KBr pellet), υ/cm^{-1}: 3370 (s), 3175 (m), 3062 (m) (ν(N(1)H+N(2)H)sym), 1547 (s), 1496 (s), ν(C=N), 1045 (s) ν(N-N), 974 (s) ν(C=S), 798 (s) and 694 (s) (thiophen ring stretchings). ^{1}H NMR (400 MHz, DMSO-d_6) δ 10.30 (s, 1H, N(2)**H**), 8.06 (s, 1H, N(1)**H**), 7.29 (d, J = 4.00, 1H, thiophen ring protons); 7.18 (d, J = 4.00, 1H, thiophen ring protons), 3.01 (d, 3H, NHC$\mathbf{H_3}$), 2.26 (s, 3H, N=CC$\mathbf{H_3}$). MALDI-TOF MS: m/z= 292 [M^+]. With slow evaporation of a saturated ethanol solution of the complex, crystals for were gathered for X-ray analysis.

2.3.3 Synthesis of 2-Acetyl-5-bromo-thiophen-N,N-dimethyl-thiosemicarbazone, TSC³

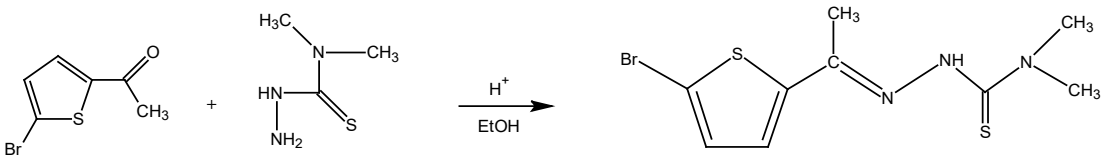

Figure 2.3 TSC³ Synthesis

2-Acetyl-5-bromothiophene (1 mol equiv) and 4,4- dimethyl -3- thiosemicarbazide (1 mol equiv) was mixed with absolute ethanol solvent (50 mL). The mixture heated up until it dissolved completely. Then concentrated sulfuric acid were added as a few drops. The solution mixed under reflux at high temperature (4 hours). After waited for cool down of solution, the TSC³ ligand acquired as a precipitate. Finally, the solution was filtrated, washed with ethanol. Then the dried in vacuo (Figure 2.3).

Light brown powder, yield: 84%. $C_9H_{12}N_3S_2Br$: Calc. %C: 38,78; H: 4,07; N: 16,96; S: 20.91. Found %; C: 38,22; H: 4,86; N: 16,75; S: 20,25. FTIR (KBr pellet), υ/cm^{-1}: 3351 (s), 3236 (m), 3165 (m) ν(N(2)H)sym, 1515 (s), 1488 (s) ν(C=N), 1064 (s) (ν(N-N), 975 (s) ν(C=S), 789 (s), 705 (s) (thiophen ring stretchings). ^{1}H NMR (400 MHz, DMSO-d_6) δ 9.65 (s, 1H, N(2)**H**), 7.34 (d, J = 3,97, 1H, thiophen ring protons); 7.20 (d, J = 3.97, 1H, thiophen ring protons), 3.22 (s, 6H, N(C**H**$_3$)$_2$), 2.31 (s, 3H, N=CC**H**$_3$). MALDI-TOF MS: m/z= 306 [M^+].

2.4 Synthesis of the Metal Complexes (general procedure)

Reactions performed under an oxygen free inert atmosphere by the thermal reactions. Every glassware were dried in oven at night (120˚C).

2 mole equivalents of TSC ligand were dissolved in dry methanol (20 mL). Then, 1 drop of HCl 37% was joined to the solution, and acidification of the reaction medium was achieved. In another schlenk, [{RuCl(η^6-*p*-cym)}$_2$(μ-Cl)$_2$] (1 mole equivalent) was dissolved in 10 mL of dry DCM and the solution was added into the TSC ligand. The reaction was continued for 24 hours under nitrogen with stirring at ambient temperature. After the reaction was terminated, a rotary evaporator was used and the volume of solution was halved. The solid was precipitated by addition of diethyl ether. The product was gathered by filtration, then dried in vacuo.

2.4.1 Synthesis of [RuCl(η^6-p-cym)(N,S-TSC^1)]Cl, {TSC^1= 5-Nitro-2-carboxyaldehydethiophen-N-methyl-thiosemicarbazone }, Complex I

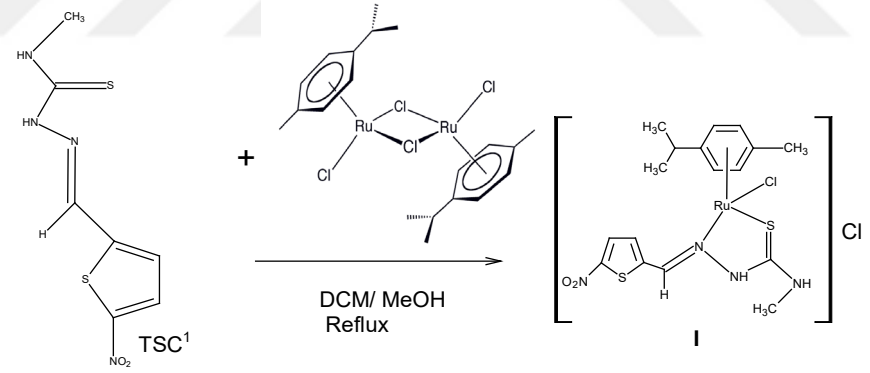

Figure 2.4 Synthesis of Complex I

5-Nitro-2-carboxyaldehydethiophen-*N*-methyl-thiosemicarbazone, (TSC^1) (2 mol eq.) and dry methanol mixed together (20 mL). After dissolving completely, 1 drop of HCl 37% added to acidify the solution. [{(η^6-p-cym)RuCl}$_2$(μ-Cl)$_2$] (1 mol eq.) and dry dichloromethane (10 ml) mixed, dissolved and added to previous solution.. The reaction continued under nitrogen at ambient temperature under stirring (24 hours). Then the rotary evaporator used to drop the volume to half. Precipitation

happened by adding diethyl ether into product solution. In the end the product obtained by filtration and dried in vacuo (Figure 2.4).

Light brown powder, yield: 62%. $RuC_{17}H_{22}N_4O_2S_2Cl_2$: Calc. %C: 24.21; H, 3.05; N, 14.12; O, 8.06; S, 16.16. Found %C: 24.02; H, 3.56; N, 14.34; O, 8.72; S, 16.24. FTIR (KBr pellet), υ/cm^{-1}: 3384 (m), 3099 (m), 3064 (m) ($\nu(N_{(1)}H+N_{(2)}H)$sym), 1576 (s), 1544 (s), ν(C=N), 1033 (s) ν(N-N), 876 (s) ν(C=S), 733 (s), 637 (s) (thiophen ring stretchings). ^{1}H NMR (400 MHz, DMSO d_6) δ 8.83 (s, 1H, **H**C=N), 8.11 (s, 1H, $N_{(2)}$**H**), 7.62 (s, 1H, $N_{(1)}$**H**), 7.12 – 7.05 (m, 2H, thiophen and 4H, p-cym ring protons), 3.07 (d, J = 4.26, 3H, NHC**H**$_3$), 2.81-2.79 (m, 1H, p-cym C**H**Me_2), 2.24 (s, 3H, p-cym C**H**$_3$), 1.18 (d, J = 5.50 Hz, 6H, p-cym CH**Me**$_2$). MALDI-TOF MS: m/z= 515 $[M-Cl]^+$; Λ_M ($\Omega^{-1}.m^2.M^{-1}$) 75.

2.4.2 Synthesis of [RuCl(η^6-p-cym)(N,S-TSC^2)]Cl {TSC^2 = 2-Acetyl-5-bromo-thiophen-N-methyl-thiosemicarbazone }, Complex II

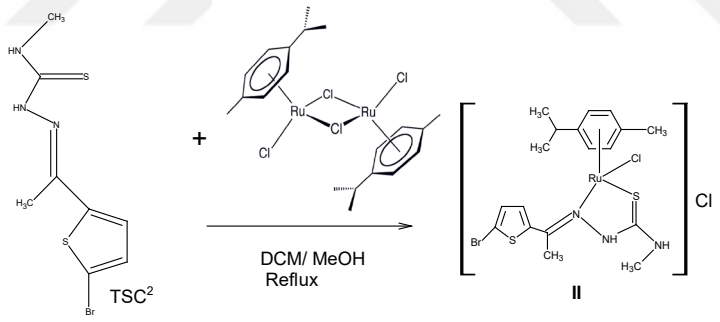

Figure 2.5 Synthesis of Complex II

2-Acetyl-5-bromo-thiophen-*N*-methyl-thiosemicarbazone, TSC^2 (2 mol eq.) and dry methanol mixed together (20 mL). After dissolving completely, 1 drop of HCl 37% added to acidify the solution. [{(η^6-p-cym)RuCl}$_2$(μ-Cl)$_2$] (1 mol eq.) and dry dichloromethane (10 ml) mixed, dissolved and added to previous solution.. The reaction continued under nitrogen at ambient temperature under stirring (24 hours). Then the rotary evaporator used to drop the volume to half. Precipitation happened by

adding diethyl ether into product solution. In the end the product obtained by filtration and dried in vacuo (Figure 2.5).

Light brown powder, yield: 53%. $RuC_{18}H_{24}N_3S_2Cl_2Br$: Calc. %C: 24.30; H, 3.17; N, 9.45; S, 14.42. Found: %C: 24.19; H, 3.12; N, 9.14; S, 14.03. FTIR (KBr pellet), υ/cm^{-1}: 3385 (w), 3162 (w), 3015 (m) (ν(N(1)H+N(2)H)sym), 1584 (s), 1564 (s) ν(C=N), 1034 (s) ν(N-N), 875 (s) ν(C=S), 789 (s), 736 (s) (thiophen ring stretchings). ^{1}H NMR (400 MHz, DMSO-d_6) δ 7.84 (s, 1H, N(2)**H**), 7.61 (s, 1H, N(1)**H**), 7.04-7.10 (m, 2H, thiophen and 4H, p-cym ring protons), 3.66 (d, J = 4.28, 3H, NHC**H**$_3$), 2.87 – 2.79 (m, 1H, p-cym C**H**Me$_2$), 2.48 (s, 3H, N=CC**H**$_3$), 2.23 (s, 3H, p-cym C**H**$_3$), 1.15 (d, J = 6.60 Hz, 6H, p-cym CH**Me**$_2$). MALDI-TOF MS: m/z= 547 $[M\text{-}Cl\text{-}Me]^+$; Λ_M ($\Omega^{-1}.m^2.M^{-1}$) 72.

2.4.3 Synthesis of [RuCl(η^6-p-cym)(N,S-TSC^3)]Cl, {TSC^3=2-Acetyl-5-bromo-thiophen-N,N-dimethyl-thiosemicarbazone}, Complex III

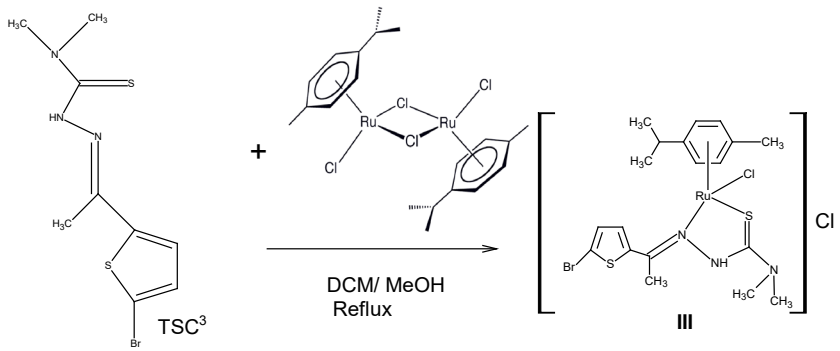

Figure 2.6 Synthesis of Complex III

2-Acetyl-5-bromo-thiophen-*N,N*-dimethyl-thiosemicarbazone, TSC^3 (2 mol eq.) and dry methanol mixed together (20 mL). After dissolving completely, 1 drop of HCl 37% added to acidify the solution. [{(η^6-p-cym)RuCl}$_2$(μ-Cl)$_2$] (1 mol eq.) and dry

dichloromethane (10 ml) mixed, dissolved and added to previous solution.. The reaction continued under nitrogen at ambient temperature under stirring (24 hours). Then the rotary evaporator used to drop the volume to half. Precipitation happened by adding diethyl ether into product solution. In the end the product obtained by filtration and dried in vacuo (Figure 2.6).

Orange powder, yield: 66%. $RuC_{19}H_{26}N_3S_2Cl_2Br$: Calc. %C: 26.18; H, 3.51; N, 9.16; S, 13.98. Found %C: 26.32; H, 3.22; N, 9.03; S, 13.25. FTIR (KBr pellet), υ/cm^{-1}: 3387 (m), 3043 (m), 2957 (s) ($\nu N_{(2)}H)_{sym}$), 1572 (s), 1535 (s) ν(C=N), 1032 (s) ν(N-N), 900 (s) ν(C=S), 800 (s), 674 (s) (thiophen ring stretchings). ^{1}H NMR (400 MHz, DMSO-d_6) δ 7.77 (s, 1H, $N_{(2)}$**H**), 7.05-7.10 (m, 2H, thiophen and 4H, p-cym ring protons), 2.77-2.80 (m, 1H, p-cym C**H**Me_2), 2.48 (s, 3H, N=CC**H**$_3$), 2.23 (s, 3H, p-cym C**H**$_3$), 2.07 (s, 6H, N(C**H**$_3)_2$), 1.16 (d, J = 5.2 Hz, 6H, p-cym CH**Me**$_2$). MALDI-TOF MS: m/z= 562 $[M\text{-}Cl\text{-}Me]^+$; Λ_M ($\Omega^{-1}.m^2.M^{-1}$) 78.

2.5 Determination and Refinement of The Crystal Structure

The crystal and molecular structures of TSC^1 and TSC^2 were elucidated by single crystal X-ray diffraction method. Rigaku-Oxford Xcalibur diffractometer with an Eos CCD area detector at 150 K has been used to collect the single-crystal data of both compounds. The graphite-monochromated MoK_α radiation (λ = 0.71073 Å) from enhanced X-ray source used for taking measurements with an ω-scan technique. CrysAlis^{Pro} program has been utilized to collect and reduce the data, as well as to handle the cell refinement. For the solution of the crystal structure and to determine the space group, we have used the ShelXT (Dolomanov, Bourhis, Gildea, Howard & Puschmann, 2009) structure solution program with Intrinsic Phasing. The "full-matrix least-squares" method on F^2 applied with SHELXL (Sheldrick, 2015) to against all reflections has been employed to refine the coordinates and anisotropic thermal parameters of non-hydrogen atoms. These calculations are carried out under crystal structure crystallographic software package OLEX2 system (Dolomanov, Bourhis,

Gildea, Howard & Puschmann, 2009). Anisotropic thermal parameters were implemented to all non-hydrogen atoms. PLATON software was used to calculation and to analyse the geometrical results (Spek, 2003). The pictures have been created by OLEX2 tools (Dolomanov, Bourhis, Gildea, Howard & Puschmann, 2009). The crystal structure of TSC^1 was concluded as a two-component twin. The final ratio of twin domains are 0.7790(6):0.2210(6). The twinning was considered during the structure refinement and data reduction using the data in HKLF5. The concise of the structure refinement, data collection and crystal data for both compounds TSC^1 and TSC^2 are displayed in (Table 3.7).

2.6 Cell Culture

The human primary ovarian cancer cell line (A2780) and the human metastatic ovarian cancer cell line (OVCAR-3) were acquired from the American Type Culture Collection (ATCC). Cells were grown in RPMI 1640 medium supplemented with 10% fetal bovine serum (FBS), penicillin (100 units/mL) and streptomycin (100 µg/mL). The cell were cultivated at 37°C in a humidified 5% CO_2 incubator.

2.7 In Vitro Cytotoxicity Assay

The antiproliferative potency of the newly synthesized TSC ligands, Ru(II) complexes and chemotherapeutic drugs (carboplatin, oxaliplatin, paclitaxel) as references were determined by the 3-(4,5-dimethylthiazol-yl)-2,5-diphenyltetrazolium bromide (MTT) assay. Stock solutions of Ru(II) complexes and TSC ligands were freshly prepared in dimethyl sulfoxide (DMSO) at 5 mM concentration. Briefly, cells reaching approximately 80% confluency were placed into 96-well plates (7500 cells/100µl/well) and waited for nearly 16-18 hours. Varying concentrations of TSC ligands (25, 50, 100 µM) and Ru(II) complexes (1, 5, 10, 50 µM) were applied to the cells for 24 hours. Then, the culture medium was taken and MTT (5 mg/mL) solution was put (100 µL/well) to each well. The plates were incubated (4 hours, 37°C). Then, MTT solution in each well was carefully discarded and Dimethyl sulfoxide (DMSO)

was placed to wells. The absorbance was obtained by using microplate reader (Thermo Multskan Go) at 540 nm. The experiments were performed in three biological replicas. IC_{50} values were defined as the drug concentration which limit cell growth at 50% ratio and IC_{50} values were calculated by using cell survival diagrams.

CHAPTER THREE
RESULTS AND DISCUSSIONS

3.1 Synthesis and Characterization of the Complexes

New ligands L= 5-nitro-2-carboxyaldehydethiophen-*N*-methyl-thiosemicarbazone, (TSC^1); 2-acetyl-5-bromo-thiophen-*N*-methyl-thiosemicarbazone, (TSC^2) and 2-acetyl-5-bromo-thiophen-*N,N*-dimethyl-thiosemicarbazone, (TSC^3) were synthesized according to described procedures and characterized by ^{1}H NMR spectroscopy, FT-IR and elemental analysis. TSC^1 and TSC^2 molecules were verified with single crystal X-ray crystallography (Figure 3.1).

Then half-sandwich arene Ru (II) compounds (I−III) of overall formula Ru[(η^6-*p*-cym)(*N,S*-TSC^{1-3})Cl]Cl were isolated as high yield. The identification of the compounds was confirmed by elemental analysis, MALDI-TOF spectrometry, ^{1}H NMR spectroscopy, FT-IR. Nevertheless, the metal binds to N, S bidentate TSC chelating ligand, a η^6-*p*-cym ring and a chloride ion at all events (Figure 3.2).

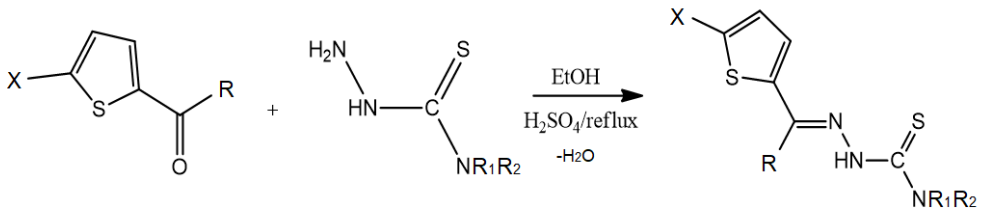

	X	R	R_1	R_2
TSC^1	NO_2	H	H	Me
TSC^2	Br	Me	H	Me
TSC^3	Br	Me	Me	Me

Figure 3.1 TSC ligands (TSC^1, TSC^2 and TSC^3)

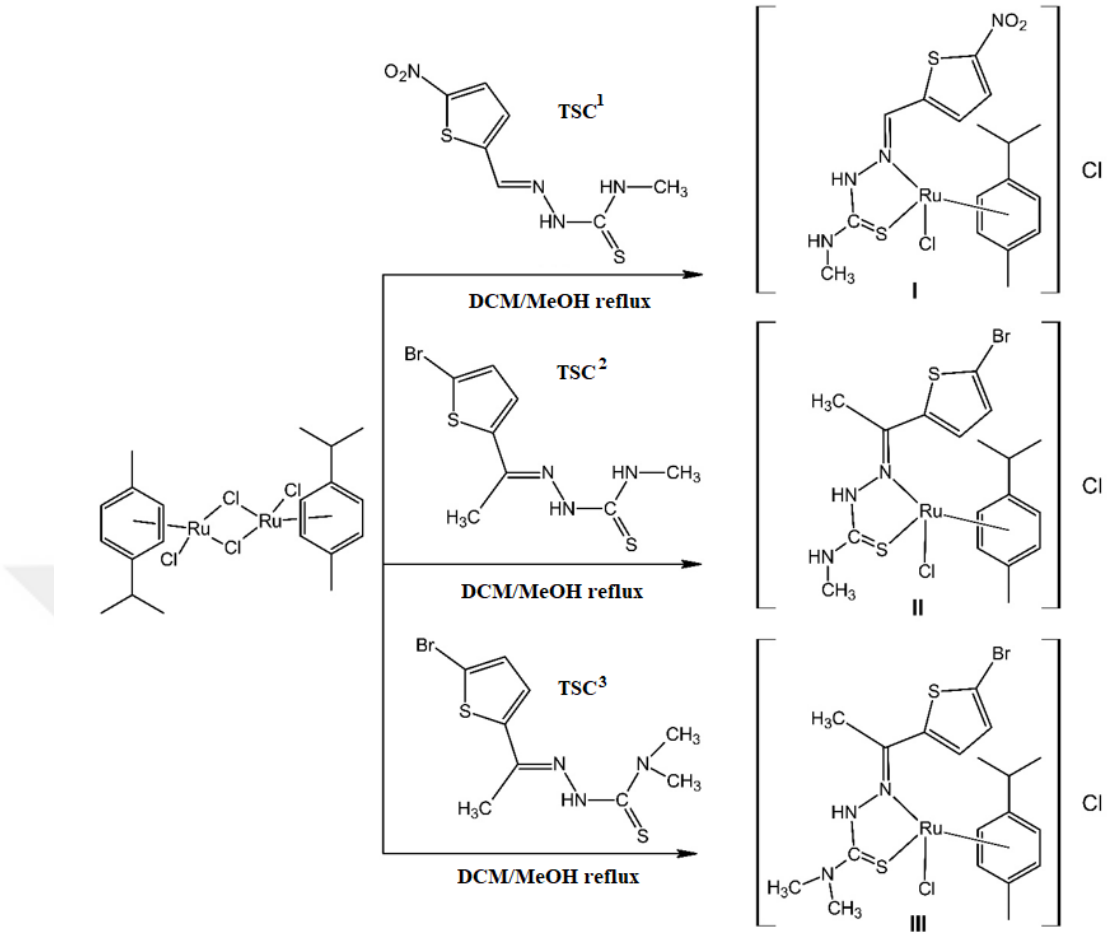

Figure 3.2 3 TSC ligands (TSC^1, TSC^2 and TSC^3) and their ruthenium complexes (I, II and III)

Ru (II) compounds have overall formula that [RuCl(η^6-p-cym)(*N,S*-TSC^1)]Cl, ***complex I***; [RuCl(η^6-p-cym)(*N,S*-TSC^2)]Cl, ***complex II*** and [RuCl(η^6-p-cym)(*N,S*-TSC^3)]Cl, ***complex III*** have been synthesised by reaction of [{(η^6-p-cymene)RuCl}$_2$(μ-Cl)$_2$] and via interested thiosemicarbazone ligands **TSC^1** (5-Nitro-2-carboxyaldehydethiophen-*N*-methyl-thiosemicarbazone), **TSC^2** (=2-Acetyl-5-bromo-thiophen-*N*-methyl-thiosemicarbazone) and **TSC^3** (2-acetyl-5-bromo-thiophen-*N,N*-dimethyl-thiosemicarbazone) with 1:2 molar ratio in methanol.

3.2 Physical Properties

Overall every compounds were purified in considerately good yields, mostly air sensitive and stable in light environment. The complexes are soluble in chloroform and dichloromethane.

According spectroscopic data and elemental analysis, it was offered that the compounds are well formulated as [(η^6-p-cym)RuCl(TSC^1)]Cl, **1**; [(η^6-p-cym)RuCl(TSC^2)]Cl, **2**; [(η^6-p-cym)RuCl(TSC^3)]Cl, **3**; (Figure 2.4, Figure 2.5, Figure 2.6). The spectroscopic data quite support the formula of the complexes.

The analytical data for new compounds are (**I-III)** showed in Table 3.1. The stoichiometry of the ligands **(TSC^1-TSC^3)** and compounds (**I-III)** have been verified with elemental analyses.

Table 3.1 Physical properties and elemental analysis datas for compounds (1-3) and the thiosemicarbazone ligands (TSC^1, TSC^2, TSC^3)

Complex	Yield	Colour	M.P.	Found /(Calcd.) (%)				
	(%)			C	H	N	S	O
TSC^1	90	Orange	246	34.42 34.82	3.30 3.17	22.93 22.66	26.25 25.85	13.10 13.87
TSC^2	85	Yellow	208	32.88 32.23	3.45 3.12	14.38 14.22	21.95 21.44	-
TSC^3	84	Light brown	187	38,78 38,22	4,07 4,86	16,96 16,75	20.91 20.25	-
I	62	Light brown	180	24.21 24.02	3.05 3.56	14.12 14.34	16.16 16.24	8.06 8.72
II	53	Light brown	172	24.30 24.19	3.17 3.12	9.45 9.14	14.42 14.03	-
III	66	Orange	168	26.18 26.32	3.51 3.22	9.16 9.03	13.98 13.25	-

3.3 Infrared Spectra

The FT-IR spectra of the thiosemicarbazone ligands and their metal Ru(II) compounds compared to investigate the binding modes of these ligands between Ru metal. The main stretching bond frequency of the FT-IR spectra of ligands TSC^n (n=**1-3**), Ru(II) compounds **I-III** are given at (Table 3.2) below.

The maximum bands frequency illustrated about 3387 cm^{-1} in the spectrum of the ligands defined as υ-sym vibration with terminal N(1)H group. This bands are also occurs in the spectra of the Ru(II) compounds **I-III** too, showing that N(1)H substituent in coordination is not involved with metal interaction (Figure 3.6 – 3.8).

The infrared spectra were presented between the range from 4000 to 650 cm^{-1}. TSCs which are shown with general formula, [R(1)R(2)C(2)=N(3)N(2)(H)C(1)=(S)N(1)R(3)R(4)] commonly coordinate to metal as either of a neutral thione form, two tautomeric forms or the anionic thiol form. The corresponding band of hydrazine N(2)–H group, propounds that the coordination of TSCs bonded with metal core (Ru) exist in a neutral thione form, not anionic thiol form (Subasi, et. al., 2020). The *ν*(C=N) stretching frequencies of the complexes (I, II and III) showed changes compared with free ligands TSC^1, TSC^2 and TSC^3 which support complexation formation. The absorptions because of (C=N) azomethine parts of thiosemicarbazone ligands at 1564, 1537 cm^{-1} **(TSC 1)**; 1547, 1496 cm^{-1} **(TSC 2)** and 1515, 1488 cm^{-1} **(TSC 3)** were founded. Coordination of the TSCs to Ru(II) through imine nitrogen is making change of electron density. This alters *ν*(C=N) azomethine band frequency (Manimaran & Jayabalakrishnan, 2012). *ν*(C=N) absorption frequencies were seen at 1576 and 1544 cm^{-1} (I); 1584 and 1564 cm^{-1} (II) and 1572 and 1535 cm^{-1} (III) in the FT-IR spectra of the compounds.

The FTIR spectra of TSC^1, TSC^2 and TSC^3 exhibited characteristic strong absorption bands attributed to thiocarbonyl (C=S) stretching, at 908, 974 and 975 cm^{-1} consecutively. They all were shifted to lower frequencies 876, 875 and 900 cm^{-1} for the complexes (I, II and III). These shifts verified that the ligand coordinated as a neutral, bidentate via imine nitrogen atoms and thiocarbonyl sulfur in (I, II and III). The *ν* (N-N) bands of TSCs were seen for ligands of **(TSC^1-TSC^3)** are 1037 cm^{-1};

1045 cm^{-1} and 1064 cm^{-1}. The decrease of the bands frequency 1033 cm^{-1} (I), 1034 cm^{-1} (II), 1032 cm^{-1} (III) confirms the coordination with the imine nitrogen (Figure 3.3 – 3.5) (Manivannan et al., 2007).

Table 3.2 Characteristic FTIR bands (cm^{-1}) of TSC^1, TSC^2, TSC^3 ligands and complexes (I, II and III).

Complex	υ(N_1H)	υ(N_2H)	υ(C=N)	υ(N-N)	υ(C=S)	υ(thiophen ring)
TSC^1	3339(s)	3142(s) 3105(s)	1564(s) 1537(s)	1037(s)	908(s)	731 (s), 694 (s)
TSC^2	3370(s)	3175(m) 3062(m)	1547(s) 1496(s)	1045(s)	974(s)	798(s), 694(s)
TSC^3	3351(s)	3236(m) 3165(s)	1515(s) 1488(s)	1064(s)	975(s)	789(s), 705(s)
I	3384(m)	3099(m) 3064(m)	1576(s) 1544(s)	1033(s)	876(s)	733(s), 637(s)
II	3385(w)	3162(w) 3015(m)	1584(m) 1564(s)	1034(s)	875(s)	789(s), 736(s)
III	3387(m)	3043(m) 2957 (s)	1572 (s) 1535(s)	1032(s)	900(s)	800(s), 674(s)

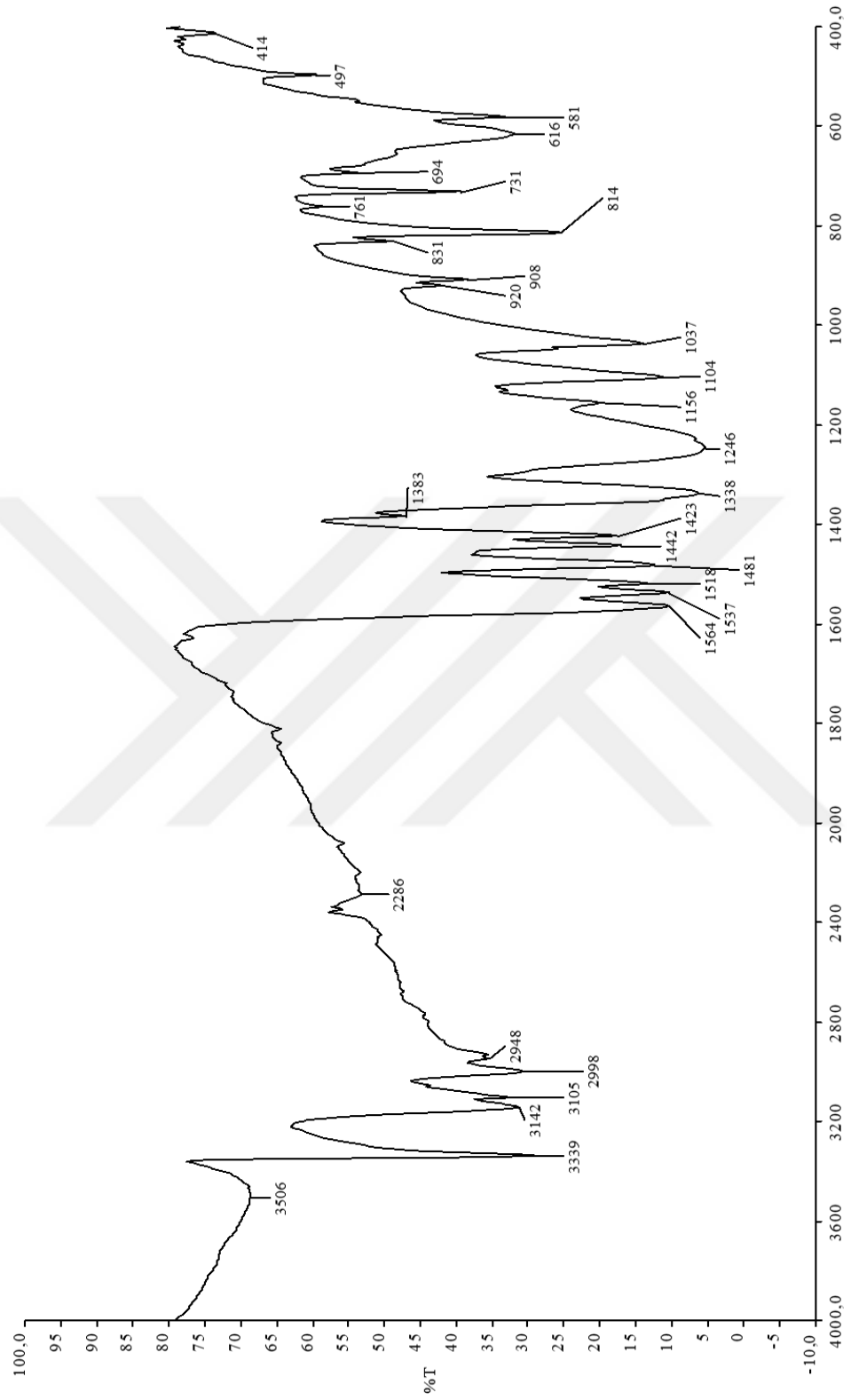

Figure 3.3 The FT-IR spectrum of TSC[1]

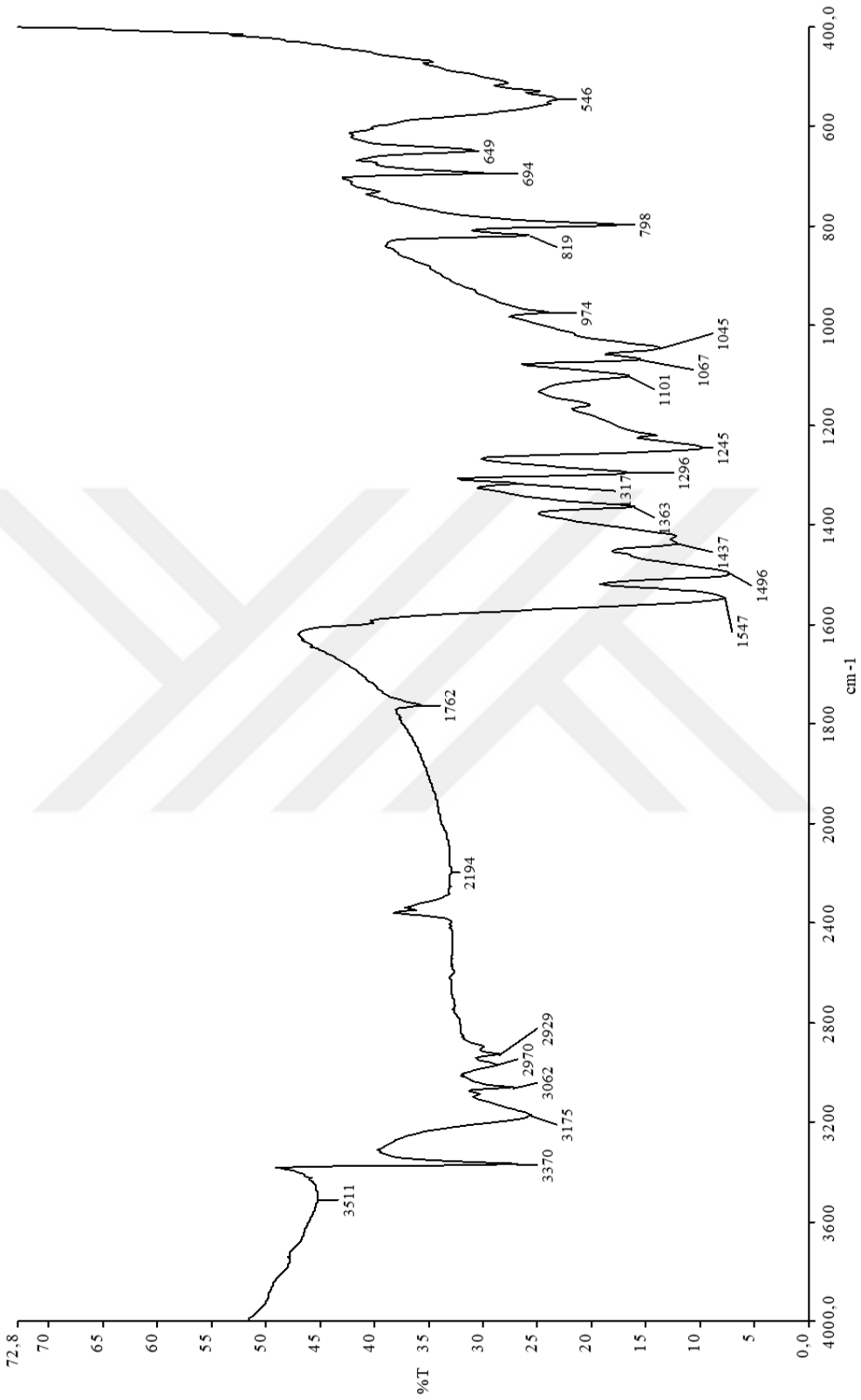

Figure 3.4 The FT-IR spectrum of TSC[2]

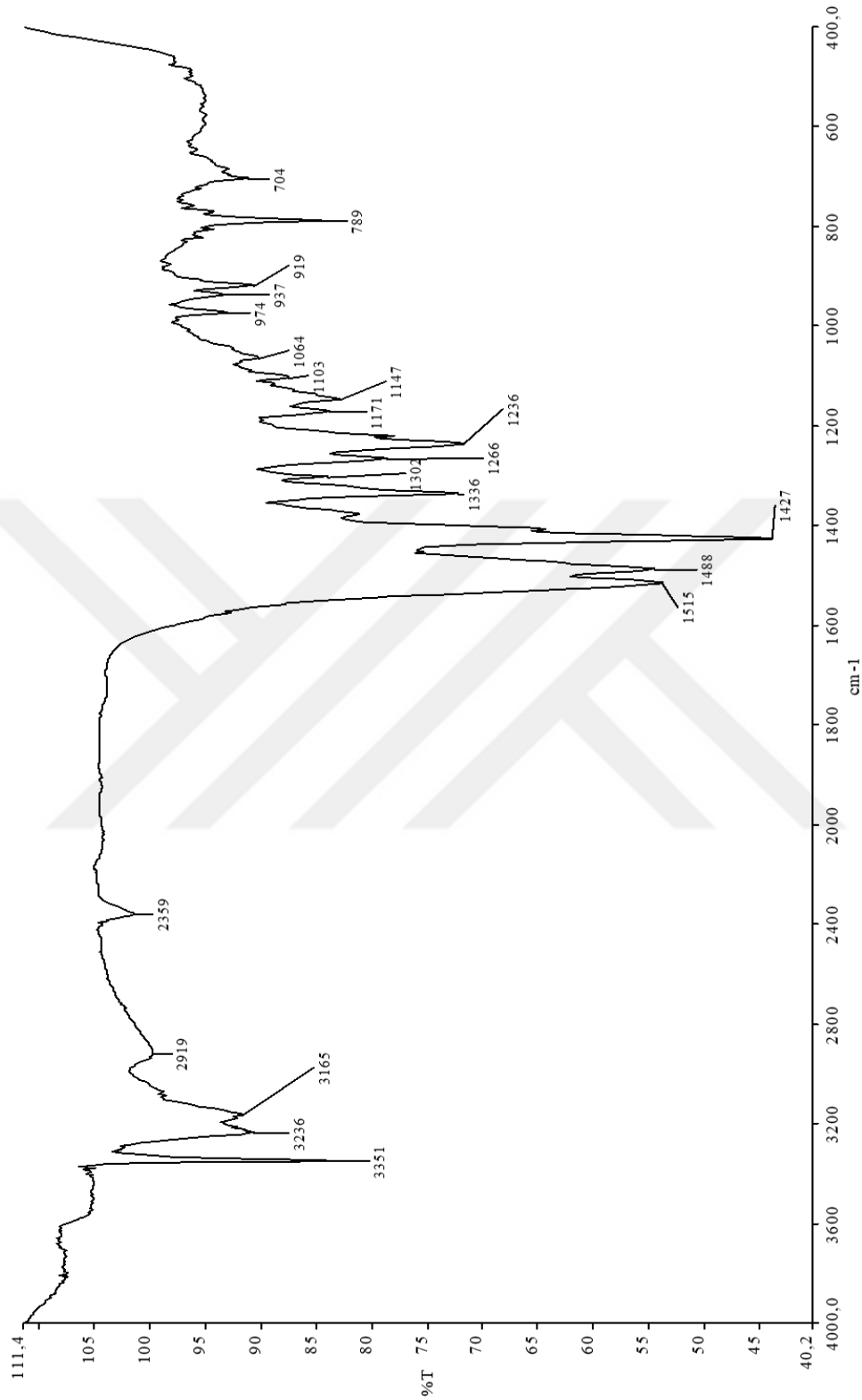

Figure 3.5 The FT-IR spectrum of TSC^3 ligand

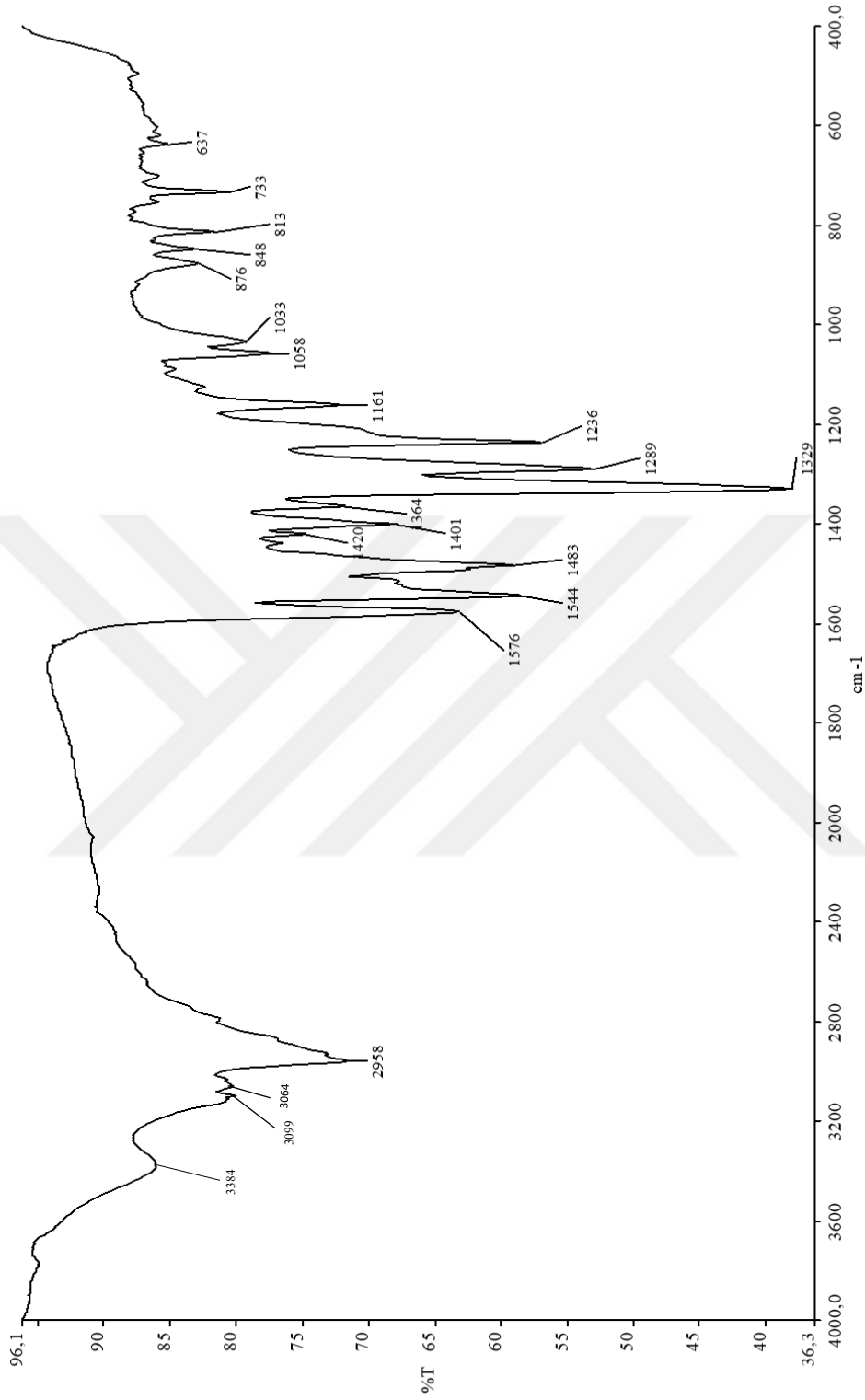

Figure 3.6 The FT-IR spectrum of complex I

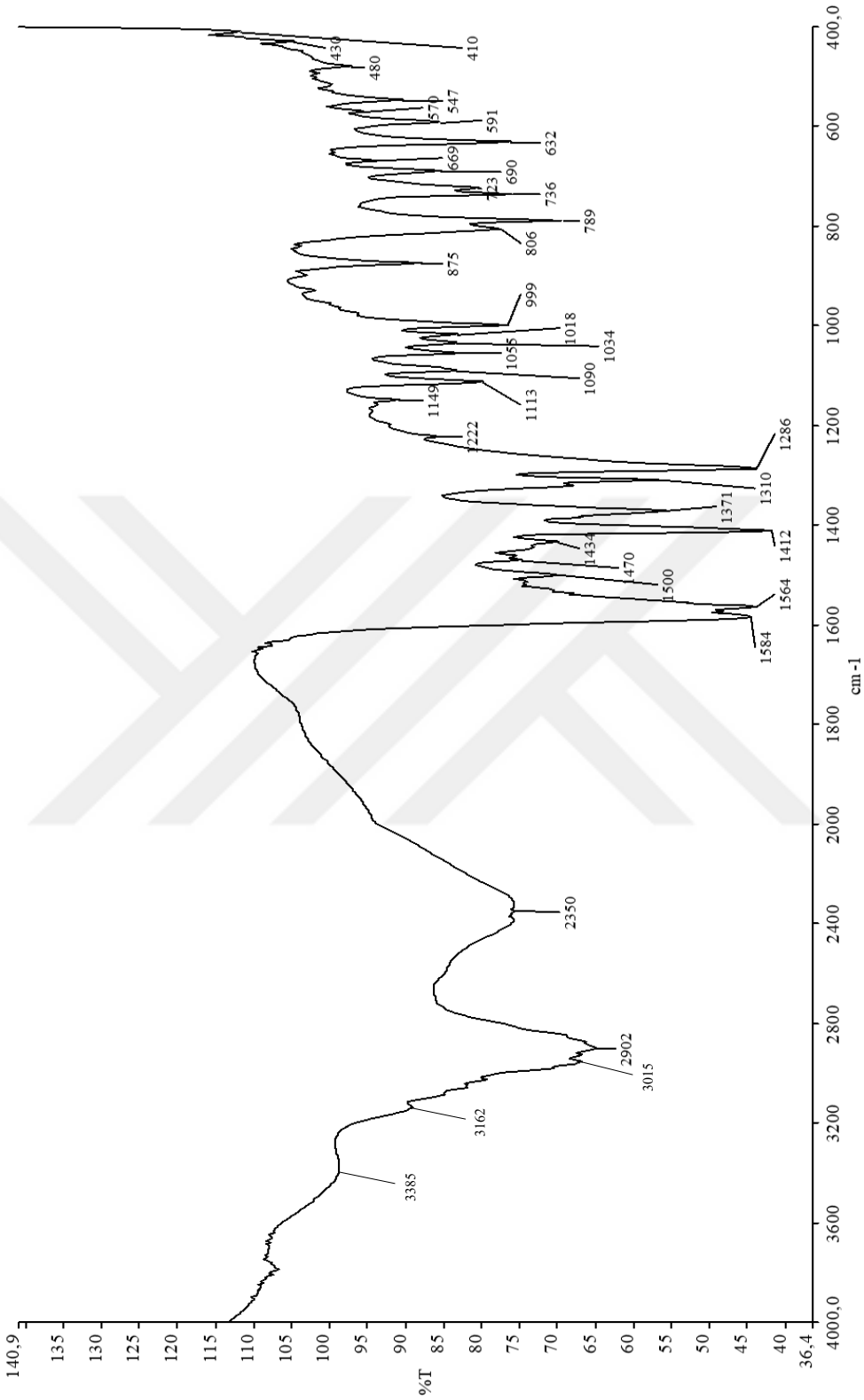

Figure 3.7 FT-IR spectrum of complex II

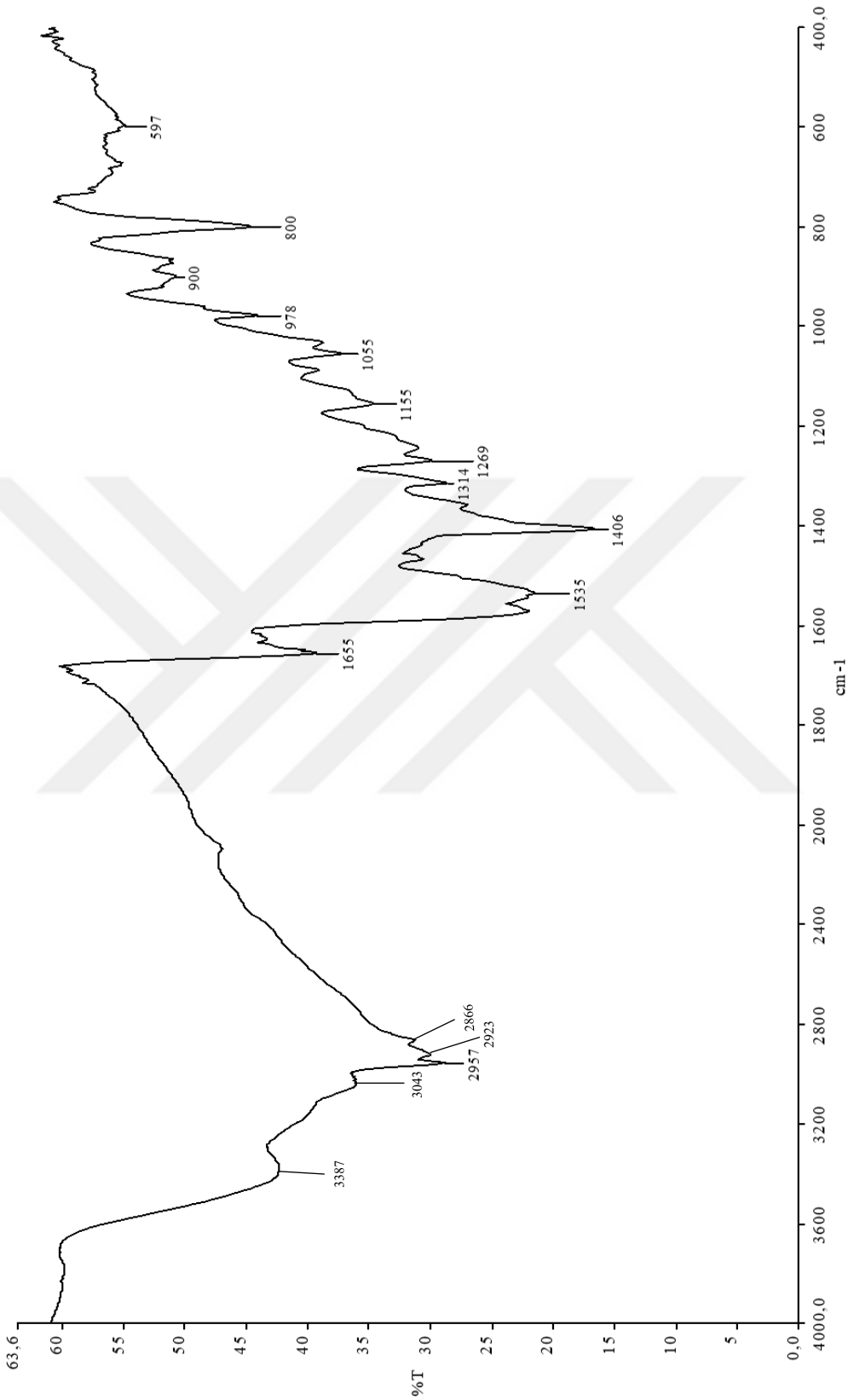

Figure 3.8 The FT-IR spectrum of complex III

3.4 ^{1}H NMR Spectra

More proof for coordinating mode of the ligands and complexes were gathered from ^{1}H NMR spectra. Sample preparation of ^{1}H NMR executed with DMSO solvent as the TSC ligands and their Ru(II) complexes are very soluble, so the spectra data were gathered in DMSO. The ^{1}H NMR spectrum data were gathered for thiosemicarbazone (**TSC^{1}, TSC^{2}, TSC^{3}**) ligands and Ru(II/III) complexes [RuCl(η^{6}-p-cym)(*N,S*-TSC^{1})]Cl, ***I***; [RuCl(η^{6}-p-cym)(*N,S*-TSC^{2})]Cl, ***II*** and [RuCl(η^{6}-p-cym)(*N,S*-TSC^{3})]Cl, ***III*** in DMSO. In the experimental section, their assignments given as well (Figure 3.9 – 3.11).

The absence of the signal at 4.00 ppm that responsible from –SH group (Das, Sinha, Britto, Somasundaram & Samuelson, 2010) shows that either solution or solid state, the ligands (TSC^{1}-TSC^{3}) exist as "thione tautomer" in the complexes (I-III).

Two sets of signals of *p*-cymene ring and the TSC protons of the coordinated ligand are seen definitely in the ^{1}H NMR spectra, L-to-M bonding is seen as well. In the spectra of (**I, II, III**) all indications shows that thiosemicarbazones remained in "neutral form" due to presence of N(2)H protons. The NH absorptions were essentially altered from that of the free TSCs in spectra (**I, II, III**). Absorptions of the free ligands N(2)H protons were observed at 8.51, (TSC^{1}); 10.30, (TSC^{2}), and 9.65, (TSC^{3}) ppm whereas upon coordination the signals were appeared at 8.11, (I); 7.84, (II), and 7.77, (III) ppm with slight highfield shifts. When comparing free TSCs with their coordinated Ru(II) ion complexes, it shows an upfield shift as the signal became more shielded. This verifies coordination of Ru(II) ion to imine nitrogen, which is also studied for many alike Ruthenium(II) TSCs compounds (Raja, Sindhuja & Ramesh, 2010; Stringer, Therrien, Hendricks, Guzgay & Smith, 2011). For complex I spectra, sharp singlet was seen at 8.83 ppm as related to azomethine proton (HC=N) and position of signal in the complex was shifted to a higher field in comparison free TSCs at 11.81 ppm (TSC^{1}), revealing coordination via the imine nitrogen. The lack of the thiol proton signal at 4.00 ppm consistent with the idea that TSCs existed as the thione tautomer in the Ru(II) compounds (I, II and III) (Das, Sinha, Britto, Somasundaram & Samuelson, 2010). The singlets because of the methyl group (CH_3C=N) in TSC^{2} and

TSC^3 spectra were observed at around 2.26 and 2.31 ppm respectively, these absorptions moved slightly towards upper field at 2.48 ppm for both of the complexes II and III.

The N(1)H singlet signals in the complexes, 7.62 ppm, (I) and 7.61 ppm, (II) attributed to the thiosemicarbazone were slightly altered to higher field from the free TSCs, 8.18 ppm, (TSC^1) and 8.06 ppm, (TSC^2). The N(1)(Me)H group generated doublets at 2.99 ppm, (TSC^1) and 3.01 ppm, (TSC^2) with a slight change in complexes at 3.07 ppm (I) and 3.03 ppm (II). Singlet resonances of NMe_2 protons in TSC^3 is at 3.22 ppm were present at 2.07 ppm in NMR spectrum of (III) with gradual upfield shifts.

The *p*-cym protons resonated at frequencies typically observed for this group (Beckford et al., 2009). The *p*-cym group have many multiplets, and thiophene ring protons were seen at near about 7.12–7.05 ppm, (I); 7.04–7.10 ppm, (II); 7.05–7.10 ppm, (III) for the complexes. The isopropyl's tertiary (3°) methine that binded *p*-cym ring was emerged as multiplets at 2.79-2.81 ppm, (I); 2,87-2.79, ppm (II); and 2.77-2.80, ppm (III), consecutively. The primary (1°) methyls binded *p*-cym ring have singlet signals at 2.24 ppm (I), 2.23 ppm (II) and 2.23 ppm (III) in sequence. The isopropyl methyl (1°) was appeared as doublets at 1,18 ppm (I), 1,15 ppm (II) and 1,16 ppm (III).

All the protons resonated in expected regions. The ^1H NMR spectra of (I, II and III) are actually direct combination of the signals from the ligands plus those from the *p*-cym moiety. In the ^1H NMR spectra of (I, II and III) all indications are that the ligands remain neutral form (Table 3.3).

Table 3.3 ^{1}H NMR data for TSC^{1}, TSC^{2}, TSC^{3} and compounds (1-3) (in DMSO solution)

Complexes Shift (ppm), class, H's, J's(Hz)	TSC^{1}	TSC^{2}	TSC^{3}	**I**	**II**	**III**
HC=N	11.81, s, 1H	-	-	8.83, s, 1H	-	-
N(2)H	8.51, s, 1H	10.30, s, 1H	9.65, s, 1H	8.11, s, 1H	7.84, s, 1H	7.77, s, 1H
N(1)H	8.18, s, 1H	8.06, s, 1H	-	7.62, s, 1H	7.61, s, 1H	-
thiophen ring and/or *p*-cym ring protons	8.05, d, J = 4.26, 1H; 7.49, d, J = 4.24, 1H	7.29, d, J = 4.00, 1H; 7.18, d, J = 3.96, 1H	7.34, d, J = 3.97, 1H; 7.20, d, J = 3.97, 1H	7.12 – 7.05, m	7.04-7.10, m	7.05-7.10, m
NHCH_3	2.99, d, J = 4.40, 3H	3.01, d, 3H	-	3.07, d, J = 4.26, 3H	3.66, d, J = 4.28, 3H	-
N=CCH_3	-	2.26, s, 3H	2.31, s, 3H	-	2.48, s, 3H	2.48, s, 3H
N(CH_3)$_2$	-	-	3.22, s, 6H	-	-	2.07, s, 6H
p-cym CHMe$_2$	-	-	-	2.81-2.79, m, 1H	2.87 –2.79, m, 1H	2.77-2.80, m, 1H
p-cym CH_3	-	-	-	2.24, s, 3H	2.23, s, 3H	2.23, s, 3H
p-cym CHMe$_2$	-	-	-	1.18, d, J = 5.50, 6H	1.15, d, J = 6.60, 6H	1.16, d, J = 5.2, 6H

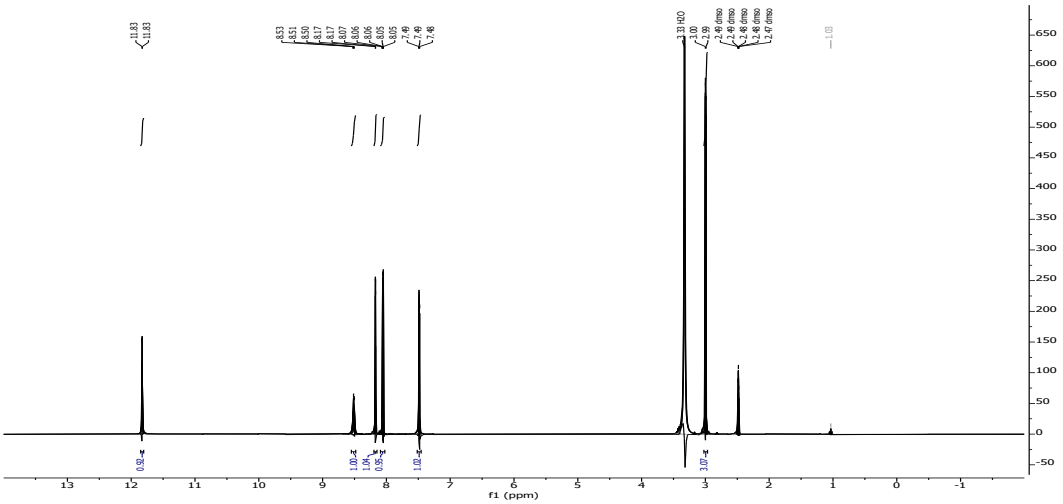

Figure 3.9 The ^{1}H NMR spectrum of TSC[1] ligand

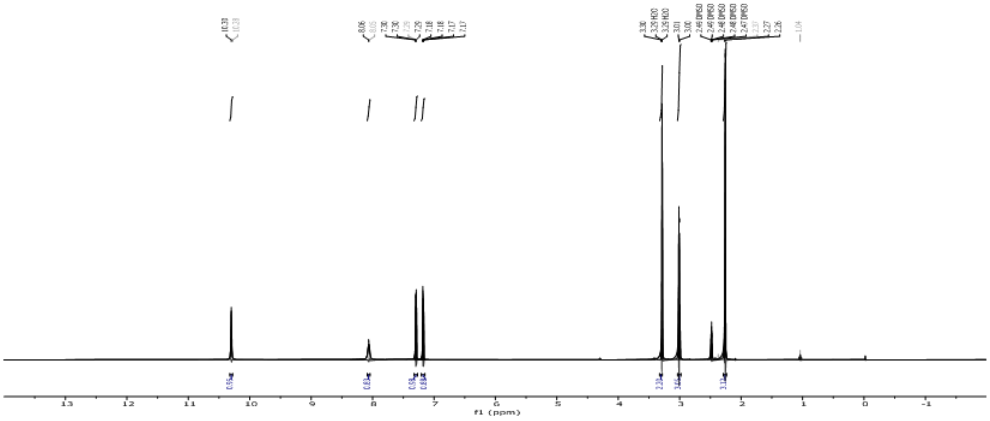

Figure 3.10 The ^{1}H NMR spectrum of TSC[2] ligand

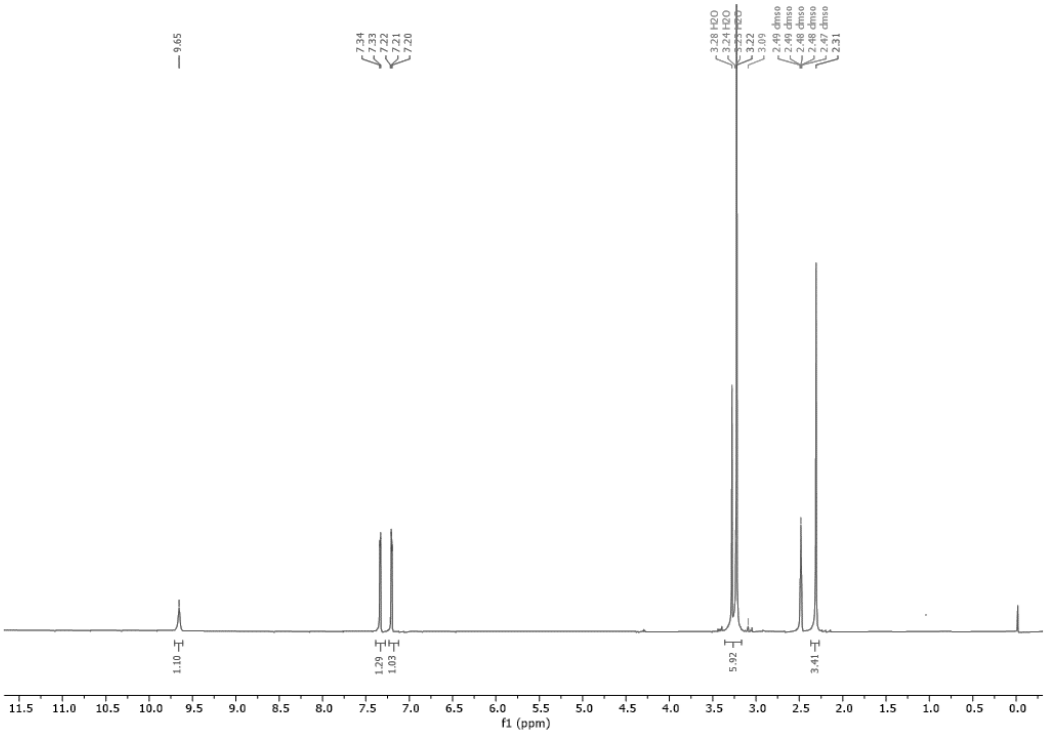

Figure 3.11 The ^{1}H NMR spectrum of TSC[3] ligand

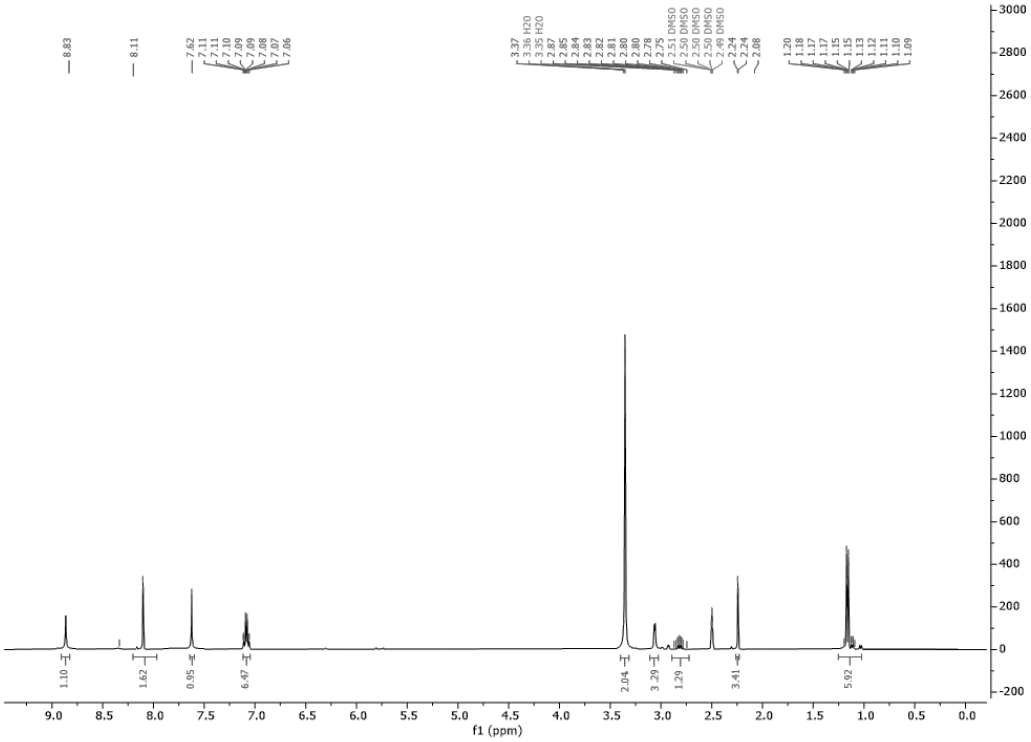

Figure 3.12 The ^{1}H NMR spectrum of complex I

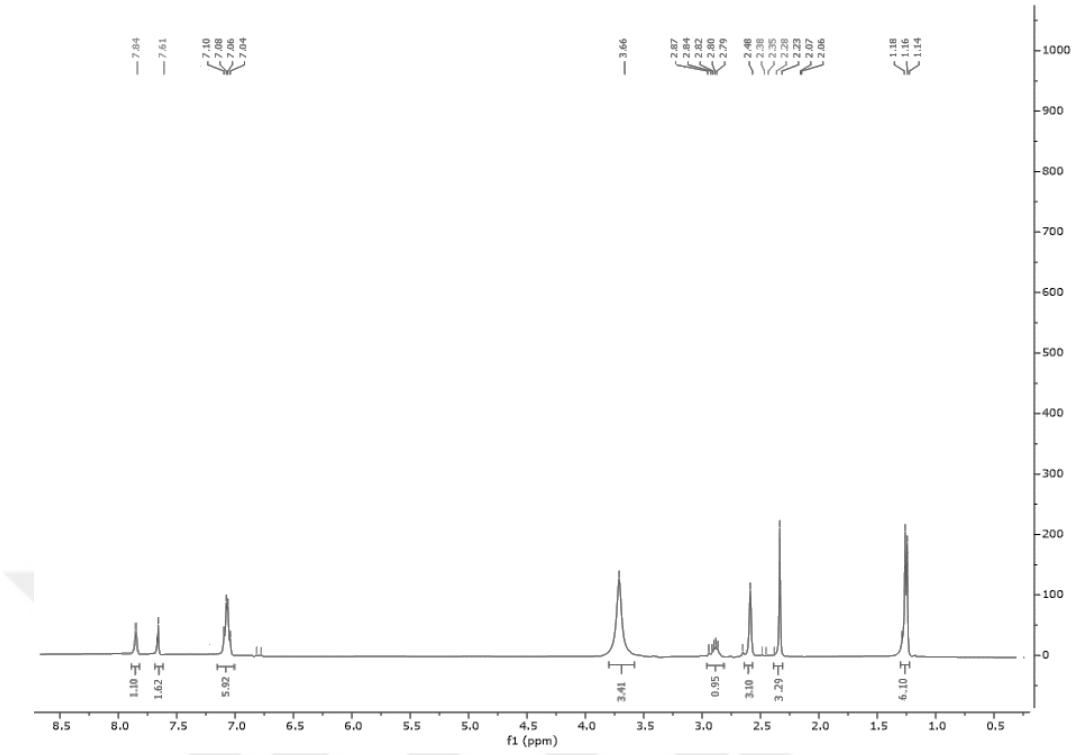

Figure 3.13 The ^{1}H NMR spectrum of complex II

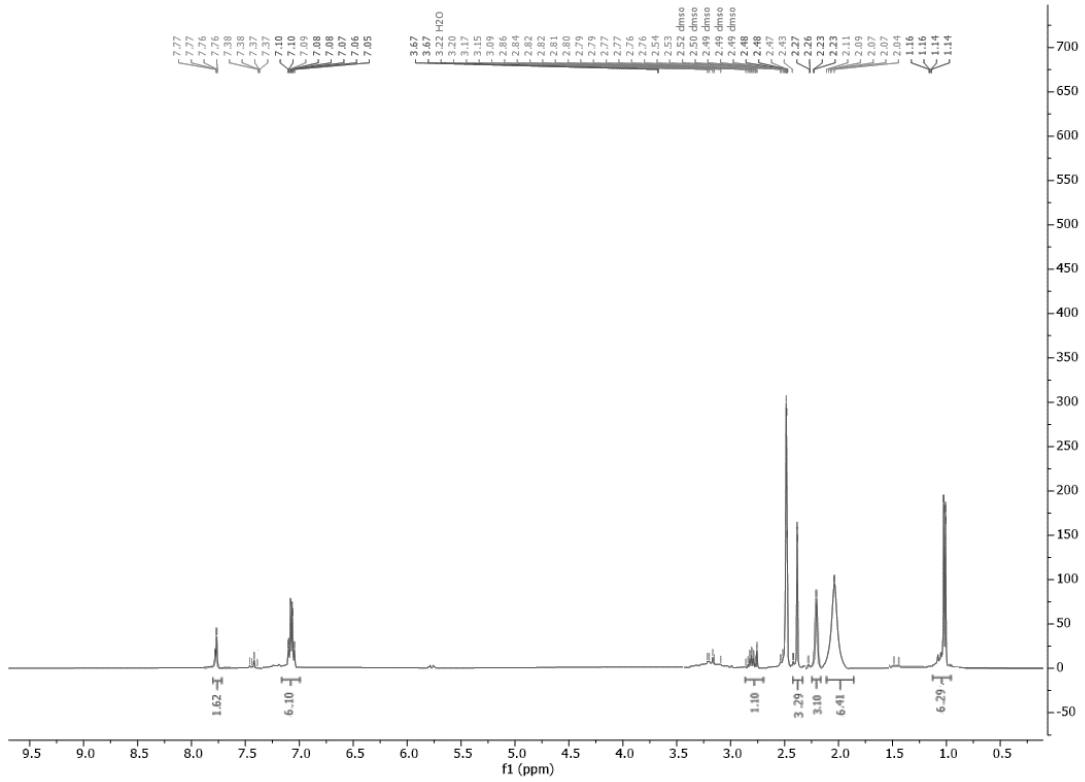

Figure 3.14 The ^{1}H NMR spectrum of complex III

3.5 Electronic Spectra

Table 3.4 The electronic spectra data for TSC^1, TSC^2 and TSC^3 ligands

	λ_{max1}(nm), A	λ_{max2}(nm), A	C (mol/L)	ε_1	ε_2
TSC^1	278.00 (0,380)	405.00 (0.554)	10^{-4}	3.80 x10^3	5.54 x10^3
TSC^2	247.50 (0.192)	337.00 (0.433)	10^{-4}	1.92 x10^3	4.33 x10^3
TSC^3	252.50 (0,730)	343.00 (0,613)	10^{-4}	7.30 x10^3	6.13 x10^3

Table 3.5 The electronic spectra data for the complexes (I-III)

	λ_{max1}(nm), A	λ_{max2}(nm), A	C (mol/L)	ε_1	ε_2
I	279.00 (0.510)	415.0 (0.442)	10^{-4}	5.10 x10^3	4.42 x10^3
II	236.00 (0.411)	337.00 (0.341)	10^{-4}	4.11 x10^3	3.41 x10^3
III	260.50 (0.267)	363.00 (0.150)	10^{-4}	2.67 x10^3	1.50 x10^3

The electronic spectra of the complexes and their ligands were obtained in ethanol. (Table 3.4 and Table 3.5) (Figure 3.15 – 3.20). The spectra of TSCs have two type of bands at 337-405 and 247-278 nm. These bands occurred likely because of n-π* (thiosemicarbazones) and π-π* (thiophene) transitions (Sharma, Singh & Tandon, 1980). A careful comparison of the bands of electronic spectral bands of complexes with those of the free ligands showed that there was little change in the energy of these bands due to extended conjugation of ligands after complexation. The ground state of Ru(II) is $^1A_{1g}$, arising from the t^6_{2g} configuration in an octahedral form. Excited state corresponding to the $t^5_{2g}e^1_g$ configuration are $^3T_{1g}$, $^3T_{2g}$, $^1T_{1g}$ and $^1T_{2g}$. A very intense band at high energy region in the electronic spectra of the complexes is reasonably assignable to a combination of ligand to metal charge transfer and metal d-d band transitions. Such observations have also been noticed earlier in other ruthenium (II) complexes of similar ligand systems. The data of electronic spectra of all complexes show that Ru(II) complexes have an octahedral geometry (Sivagamasundari & Ramesh, 2007).

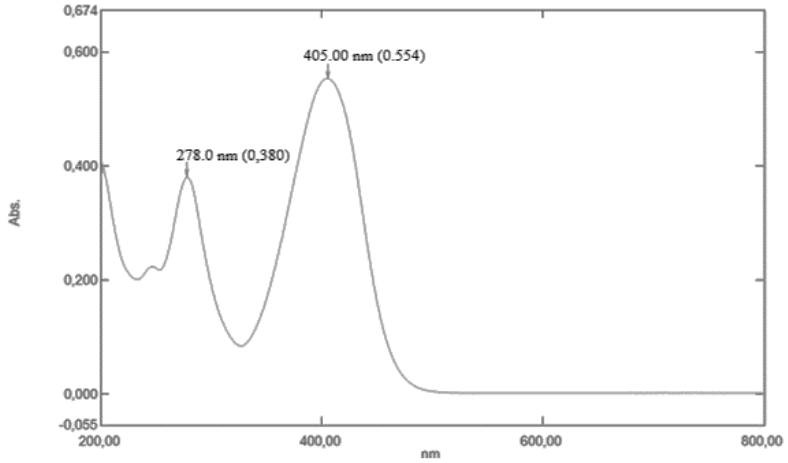

Figure 3.15 The UV-Vis spectrum of TSC[1] ligand

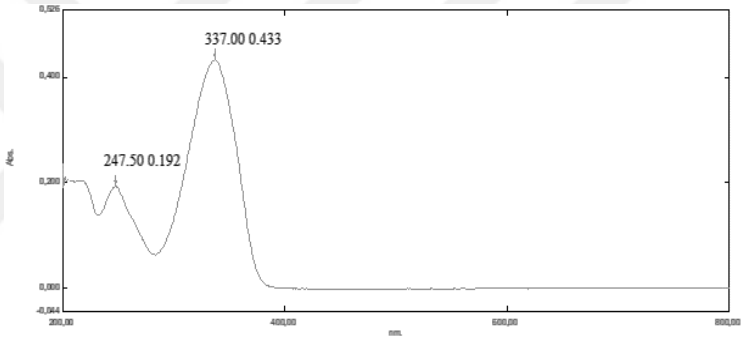

Figure 3.16 The UV-Vis spectrum of TSC[2] ligand

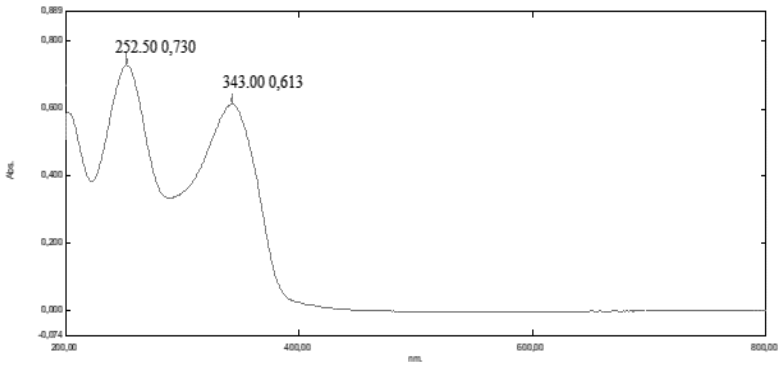

Figure 3.17 The UV-Vis spectrum of TSC[3] ligand

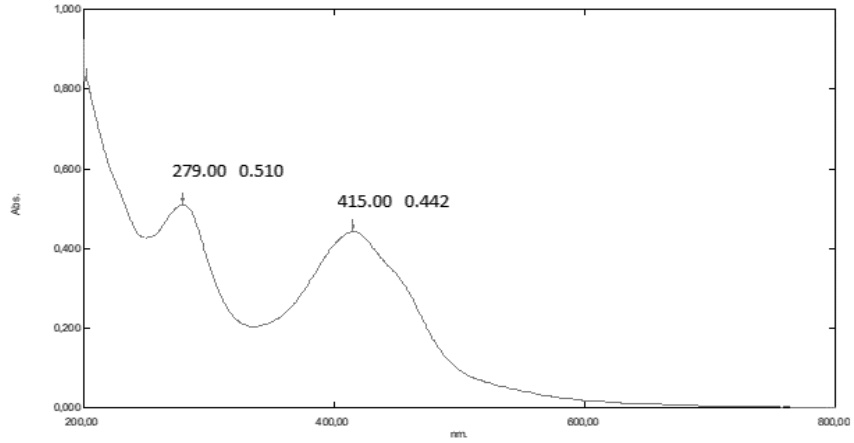

Figure 3.18 The UV-Vis spectrum of complex I

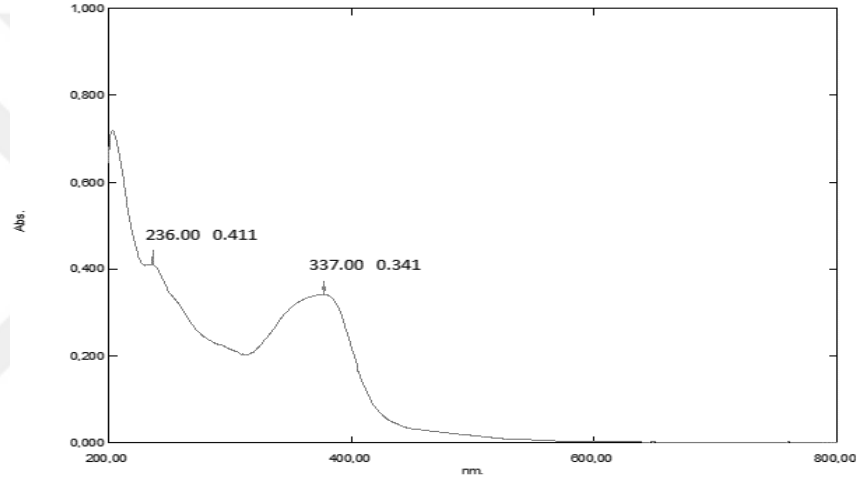

Figure 3.19 The UV-Vis spectrum of complex II

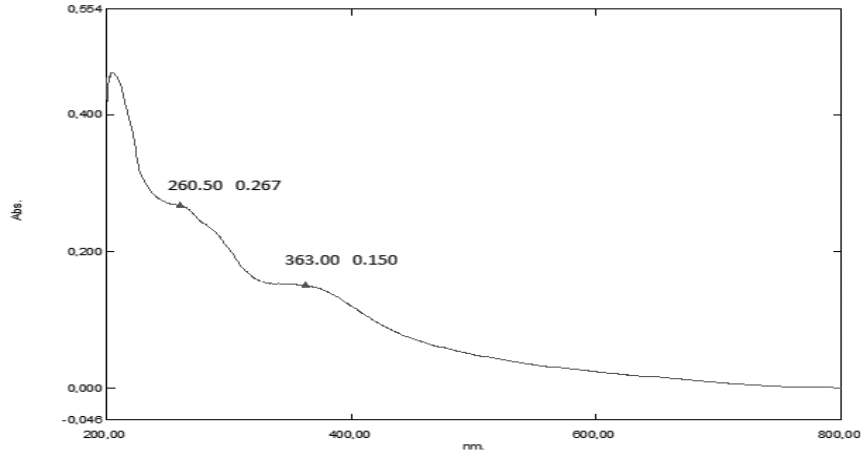

Figure 3.20 The UV-Vis spectrum of complex III

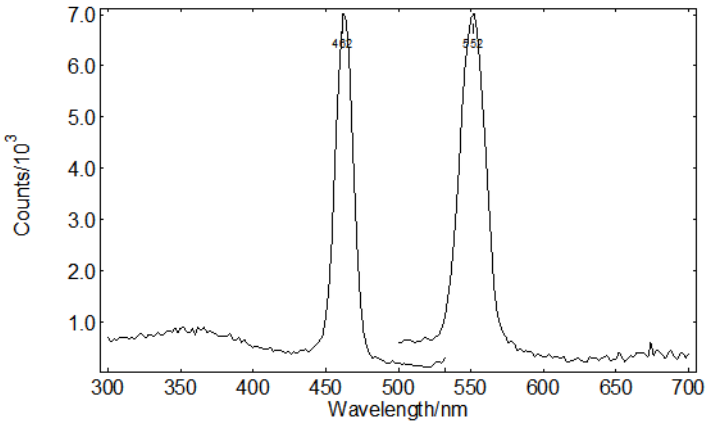

Figure 3.21 Excitation-emission spectra of the 1.10^{-5} M Ru complex (I) solutions in THF (λ_{ex}=462 nm λ_{em}=552 nm).

The complex (I) exhibited very sharp and narrow band excitation and emission peaks when excited at 462 nm. The less intense and broad excitation peak centered around 360 nm can be assigned to the $\Pi \rightarrow \Pi^*$ transitions within the ligand where the conjugate system continues for only 3 bonds. However the intense and sharp excitation peak centered at 452 nm arises from the "metal-to-ligand charge transfer (MLCT)" effect in the Ru(II) complex (Figure 3.21).

The Stokes shift ($\Delta\lambda$) of 90 nm has been extracted which manifests the adaptation ability of the presented Ru(II) complex for the potential "fluorescent dye applications".

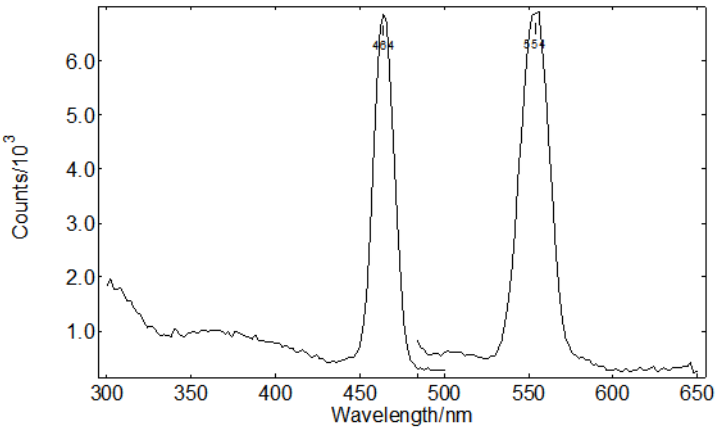

Figure 3.22 Excitation-emission spectra of the 1.10^{-5} M Ru complex (II) solutions in THF (λ_{ex}=464 nm λ_{em}=554 nm).

Substitution of the electron withdrawing -NO_2 group with the inductively withdrawing -Br in the complex (II) resulted in 2 nm of red shifted excitation maximum for the complex. However, the emission maximum shifted only 2 nm towards the red side without a significant change in the shape of the emission spectrum (Figure 3.22).

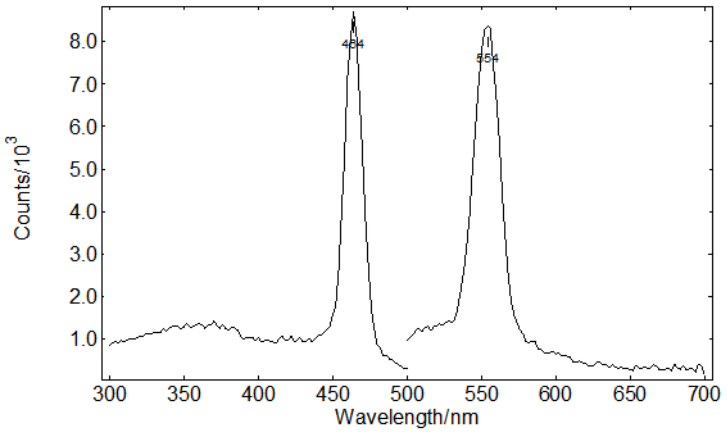

Figure 3.23 Excitation-emission spectra of the 1.10^{-5} M Ru complex (III) solutions in THF (λ_{ex}=464 nm λ_{em}=554 nm).

Substitution of the –$NHCH_3$ in the complex (II) with the electron donating dimethylamino in the complex (IV) did not cause a spectral differentiation on either the excitation or emission side. This may be due to the fact that the dimethylamino group is far from the conjugate system in the ligand and does not participate in the conjugation (Figure 3.23).

3.6 Mass Spectra and Conductivity Measurements

Table 3.6 MALDI-TOF Mass Spectra Data

	m/z
TSC[1]	244 [M^+]
TSC[2]	292 [M^+]
TSC[3]	306 [M^+]
Complex I	515 [M - Cl]$^+$
Complex II	547 [M-Cl-Me]$^+$
Complex III	562 [M-Cl-Me]$^+$

The MALDI-TOF mass spectra of the TSCs and the complexes proved the suggested structures. Exact molecular ion peaks were observed for the ligands at 244 m/z (TSC^1), 292 m/z (TSC^2), 306 m/z (TSC^3). However, according to the mass analysis of the complexes the peaks at 515 m/z (I), 547 m/z (II) and 562 m/z (III) were equal to the total molecular weight of $[M\text{-}Cl]^+$, (I); $[M\text{-}Cl\text{-}Me]^+$, (II); $[M\text{-}Cl\text{-}Me]^+$, (III). The chloride ion loss confirmed all the complexes have chloride ion as counter ion (Table 3.6), (Figure 3.24 – 3.29).

The complexes I-III have molar conductance (10^{-3} M in DMSO) in the range of 72–78 Λ_M (Ω^{-1}. m^2. M^{-1}) at 38°C suggesting 1:1 electrolytic behaviour (Ali, Wani & Saleem, 2013)

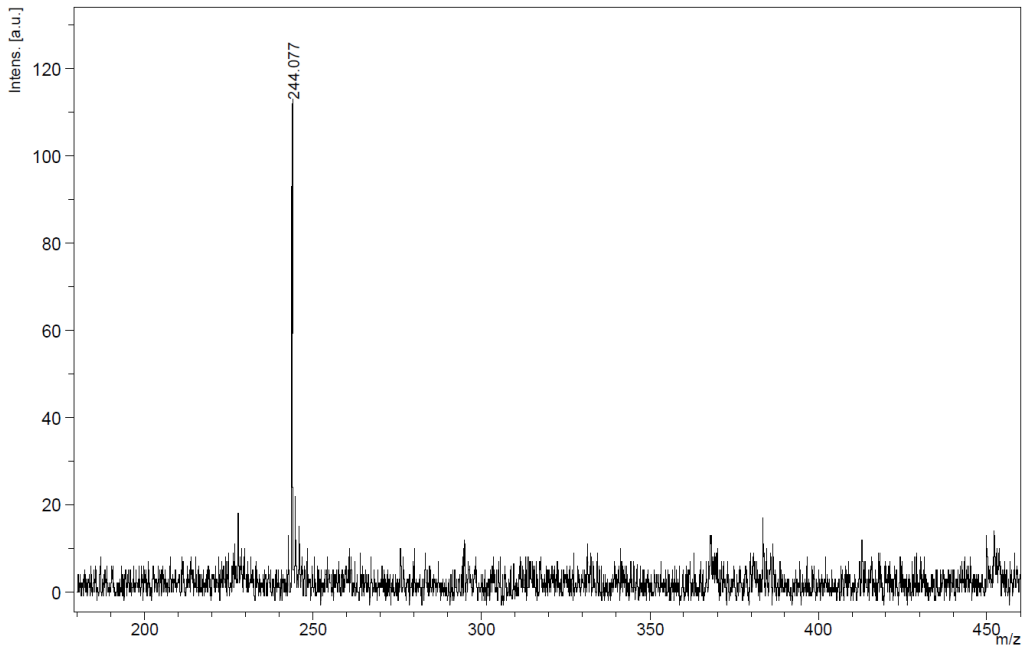

Figure 3.24 TSC^1 mass spectrum

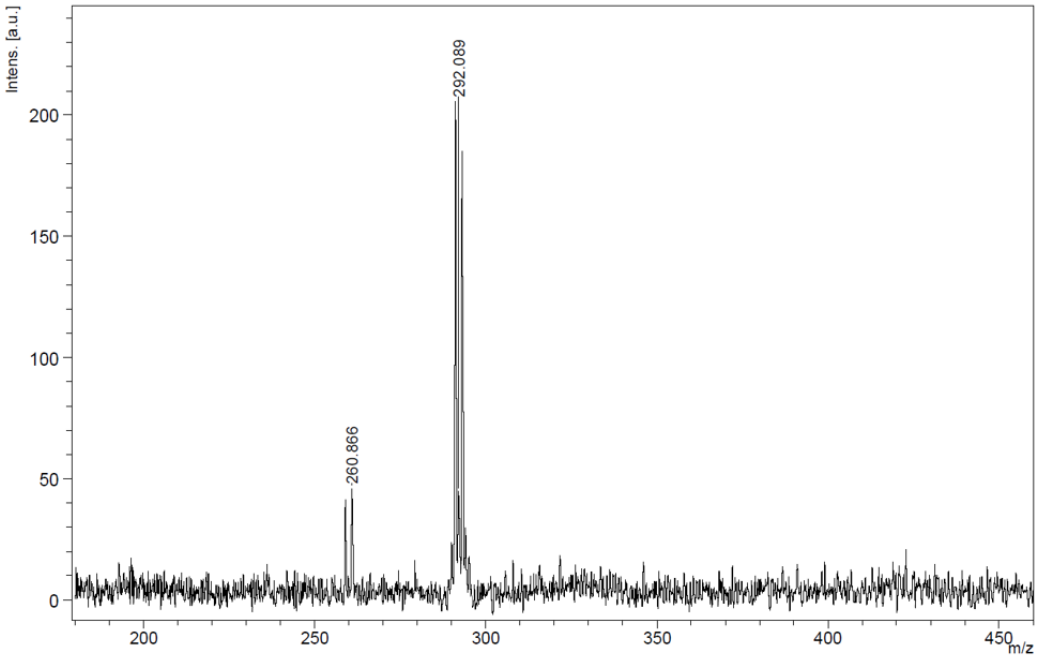

Figure 3.25 TSC^2 mass spectrum

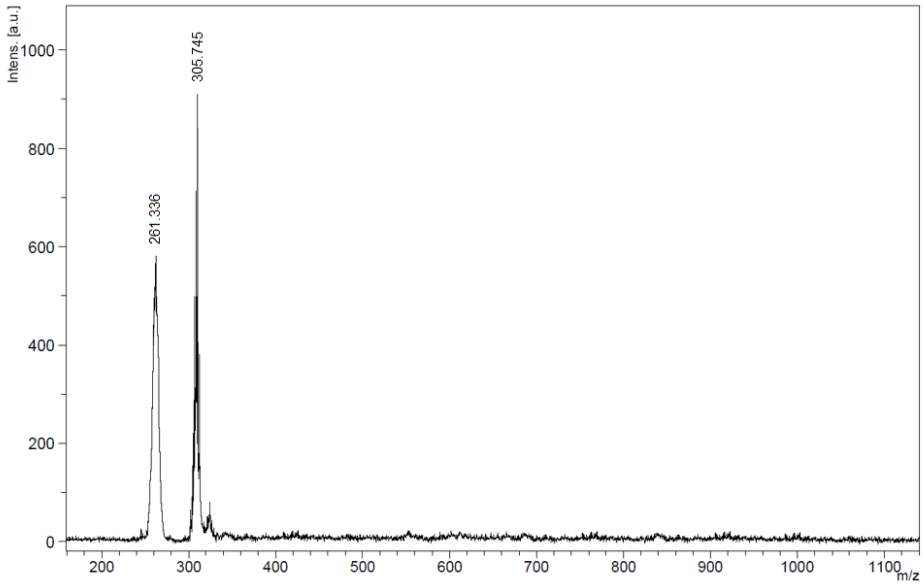

Figure 3.26 TSC^3 mass spectrum

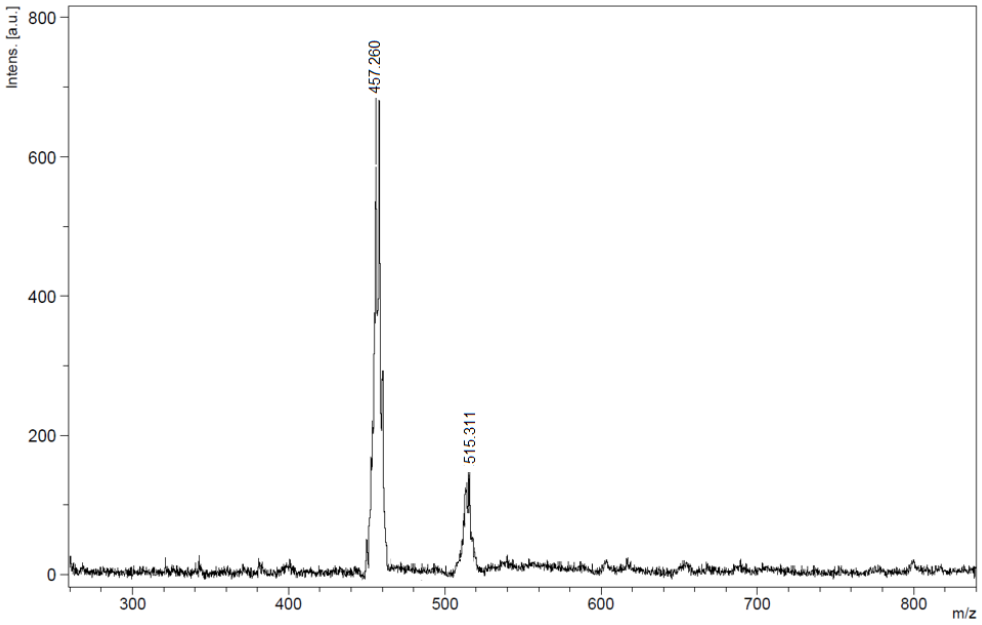

Figure 3.27 Mass spectrum of complex I

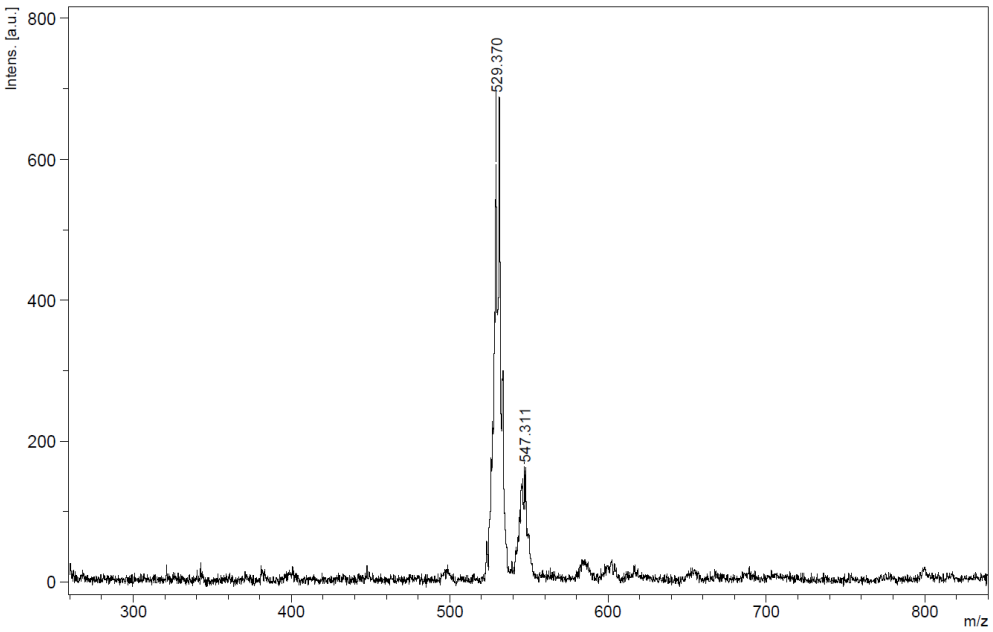

Figure 3.28 Mass spectrum of complex II

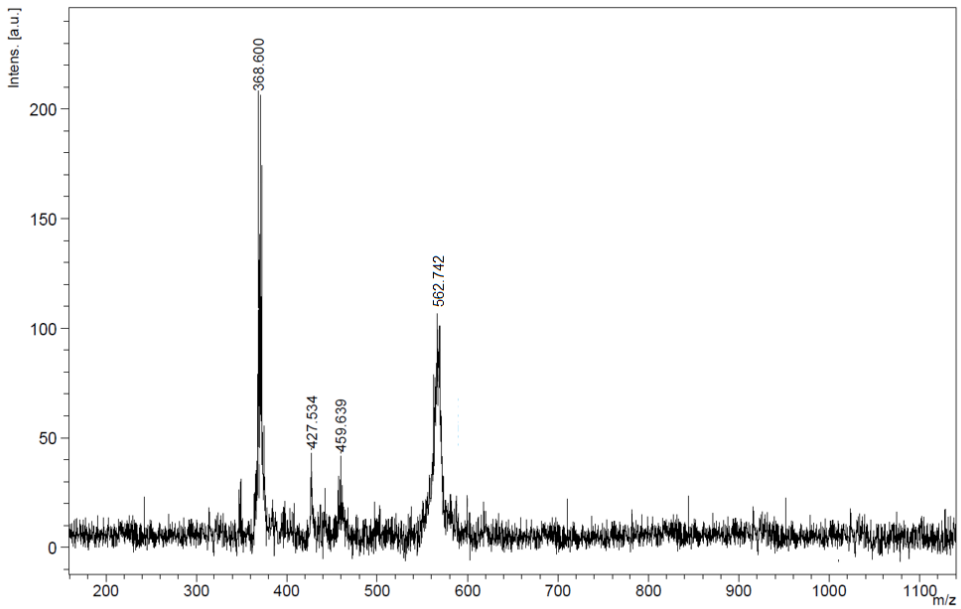

Figure 3.29 Mass spectrum of complex III

3.7 Structural Description of Compounds TSC1 and TSC2.

Both ligand compounds TSC[1] and TSC[2] crystallized in the triclinic crystal system with space group P-1, and their molecular structures are depicted (Table 3.7). There are small differences between both compounds in the bond lengths and angles as shown in Table 3.8.

It is well known that thiosemicarbazones can show thione–thiol tautomerism due to the presence of thioamide functional group (Nehar, Louhibi, Boukli-Hacene & Roisnel, 2016; Zhang, Wu, Zhuang & Wang, 2009). S–C and C–N bond lengths have supported that both compounds appear as a thione form. The exocyclic S–C bond distances are 1.686 (3) Å in compound TSC[1] and 1.682 (4) Å in compound TSC[2], and can be compared with those corresponding to some other related complexes (Parsons, Smith, Tasker & White, 2000; Latheef, Manoj & Prathapachandra, 2006; Trinajstić, 1968). These bond lengths lie between the values of isolated single (C–S) and double bond (C=S) (1.82 and 1.56 Å, respectively) (Trinajstić, 1968), showing a partial double bond character (Miroslaw, Szulczyk, Koziol & Struga, 2011) due to electron

delocalization. On the other hand, C2–N2 bond distances are more or less the same for both compounds, and these distances are of single-bond character (Table 3.8). Similar values for C–N bond lengths are also observed for related compounds in the literature (Trinajstić, 1968; McBurney, Crundwell, Updegraff III, Zeller & Hunter, 2005; Latheef, Manoj & Prathapachandra, 2006).

Both of compounds TSC^1 and TSC^2 are is close to planar with the greatest deviation from the mean plane being 0.133 (3) at O1 and −0.236 (3) Å at C1, respectively. However, the 5-nitro thiophene ring in TSC^1 [5-bromo thiophene ring in TSC^2] and thiosemicarbazone fragment of molecule were twisted concerning for to one another doing "dihedral angle", 4.24(6)° [9.085(1)°] (Table 3.7).

N4–O1 and N4-O2 bond lengths are 1.221(3) and 1.236(3) Å in compound TSC^1, which are in agreement with bond length reported for other compounds of 5-nitrothiophene (Ceylan, Tanak, Gümüş & Ağar, 2011; Köysal, Bülbül, Gümüş, Ağar & Soylu, 2016; Pappenfus, Wood, Morey, Wilcox & Janzen, 2018). The Br1–C7 "bond length", 1.874(3) Å is normal and found in literature (Bernstein, Davis, Shimoni & Chang, 1995; Li, H., & Li, L., 2009; Geiger, H. C., Donohoe & Geiger, D. K., 2014).

In the crystal packing of compounds TSC^1 and TSC^2, intermolecular interactions construct centrosymmetric dimeric motifs but give different supramolecular architecture. An S(5) ring motif is generated due to cyclic intramolecular N1–H1···N3 hydrogen bonds which supports the molecular conformation of both compounds (Halfpenny & Sloman, 2000).

In the crystal structure of TSC^1, C6 atom act as hydrogen bond donor to O2 atom of an inversion-related molecule, producing an $R_2^2(10)$ hydrogen-bonded dimer through C6–H6···O2 hydrogen bond. Additionally, a pair of N1–H1···O1 and C1–H1C···O2 interactions constitutes a cyclic dimer with an $R_2^2(7)$ loop while N1–H1···O1 hydrogen bond also generates inversion dimer enclosing $R_2^2(22)$ rings. This dimer linkage is connected by another dimer-set which is linked via couple of N2–H2···S1 "hydrogen bonds", forming centrosymmetric dimer with an $R_2^2(8)$ ring motif. The molecules are formed a two-dimensional hydrogen bonded network extending parallel to $(1\bar{1}2)$ through these intermolecular interactions. Furthermore, these aforementioned dimers are stacked by intermolecular N4–O2···Cg (Cg is the centroid

of thiophene ring) interactions along the diagonal of (110) plane, giving an overall three-dimensional structure (Figure 30 – 32).

In the crystal of compound TSC[2], N2–H2···S2 hydrogen bond pairs give inversion dimer with a $R_2^2(8)$ ring motif, leading to stairs aligned parallel to the (110) plane. The dimers are arranged in layers and are stacked into the crystallographic *b*-axis direction by π–π interaction [Cg···Cg^{ij}=3.916(2) Å, inter-planar distance= 3.529(1) Å, slippage 1.697 Å, where Cg is the center of gravity of thiophene ring; symmetry code: (***jj***) 1-x,1-y,1-z] (Table 3.9). In addition, Br1···S1 inter-ligand distance is 3.4577 (3) Å which is much shorter than the corresponding expected van der Waals radii sum of 3.70 Å (Koziol, A. E., Palenik, R. C., & Palenik, G. J, 1988). Hence, these distances may denote the presence of nonbonding intermolecular interactions. These interactions align the molecules along the diagonal line of the *b* and *c* axes. For both compounds, a detailed information of the intra- and intermolecular interactions is given in Table 3.9.

Table 3.7 Crystal data and refinement parameter for complexes TSC[1] and TSC[2].

	TSC[1]	TSC[2]
Chemical formula	$C_7H_8N_4O_2S_2$	$C_8H_{10}BrN_3S_2$
Formula weight	244.29	292.22
Temperature (K)	150.01(10)	150.01(10)
Space group	P-1	P-1
Crystal system	Triclinic	Triclinic
a (Å)	4.4615(6)	7.1576(5)
B (Å)	9.4095(13)	7.6088(7)
c (Å)	13.137(2)	11.7561(11)
α (°)	72.024(14)	93.901(8)
β (°)	82.613(13)	99.191(7)

Table 3.7 Continues

γ (°)	77.432(12)	116.951(8)
Cell volume (Å^3)	510.89(13)	556.16(8)
Formula unit cell Z	2	2
ρ_{calc} (g/cm^3)	1.588	1.745
F(000)	252.0	292.0
μ (mm^{-1})	0.506	4.035
Crystal size (mm^3)	0.484×0.089×0.039	0.506×0.386×0.225
Diffractometer	Xcalibur, Eos	Xcalibur, Eos
Radiation/Wavelength (Å)	MoK_α/0.71070	MoK_α/0.71070
Reflections measured	2669	2988
Range of *h, k, l*	$-5 \leq h \leq 5$	$-8 \leq h \leq 8$
	$-11 \leq k \leq 11$	$-8 \leq k \leq 9$
	$-16 \leq l \leq 15$	$-14 \leq l \leq 10$
Data/restraints/parameters	2669/0/138	2103/0/129
Final R indexes [I>=2σ (I)]	R_1= 0.0456, wR_2= 0.0589	R_1= 0.0357, wR_2=0.0727
Final R indexes [all data]	R_1= 0.0809, wR_2= 0.0633	R_1= 0.0443, wR_2= 0.0764
Goodness-of-fit on F^2	0.823	1.027
Largest diff. Peak/hole (e Å^{-3})	0.32/-0.29	0.55/-0.51

Table 3.8 Selected bond lengths and angles (Å,°) for the compounds TSC^1 and TSC^2.

	TSC^1	TSC^2
S2–C7	1.713(3)	1.720(4)
S2–C4	1.726(3)	1.740(3)
S1–C2	1.686(3)	1.682(4)
N1–C2	1.312(3)	1.321(4)
N2–C2	1.360(3)	1.358(4)
N3–N2	1.366(3)	1.381(4)
C5–C6	1.405(4)	1.407(5)
N1–C2–N2	117.2(3)	116.9(3)
C3–C4–S2	121.8(2)	120.4(3)
S2–C7–N4 / Br1	119.7(2)	120.3(2)
C4–S2–C7	89.2(1)	90.8(2)
C3–C4–C5	125.6(3)	129.6(3)

Table 3.9 Hydrogen-bond geometry for compounds TSC^1 and TSC^2 (Å, °).

D – H ··· *A*	*D* – H	H ··· *A*	*D* ··· *A*	*D* – H ··· *A*
Compound TSC¹				
N1–H1···N3	0.86	2.29	2.657(3)	106
C6–H6···O2^{i}	0.93	2.43	3.336(3)	164
N1–H1···O1^{ii}	0.86	2.38	3.195(3)	158
C1–H1C···O2^{ii}	0.96	2.47	3.340(4)	150
N2–H2···S1^{iii}	0.86	2.54	3.362(2)	159
N4–O2···Cg^{iv}	1.236	3.656	4.010(3)	97.5
Compound TSC²				
N1–H1···N3	0.86	2.22	2.608(5)	107
N2–H2···S1^{j}	0.86	2.74	3.423(3)	137

Symmetry transformations used to generate equivalent atoms: (***i***) -x,-y,1-z; (***ii***) 1-x,1-y,1-z; (***iii***) 3-x,1-y,-z; (***iv***) -1+x,y,z; (***j***) 2-x,1-y,2-z

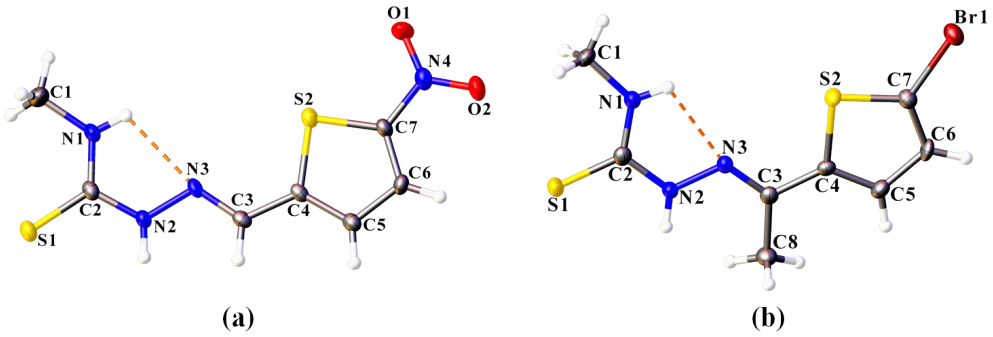

Figure 3.30 The molecular structure of compounds (a) TSC[1] and (b) TSC[2], with displacement ellipsoids drawn at the 50% probability level. The intramolecular N–H···N hydrogen bond is shown as orange dashed lines. H atoms are represented as small spheres of arbitrary radii.

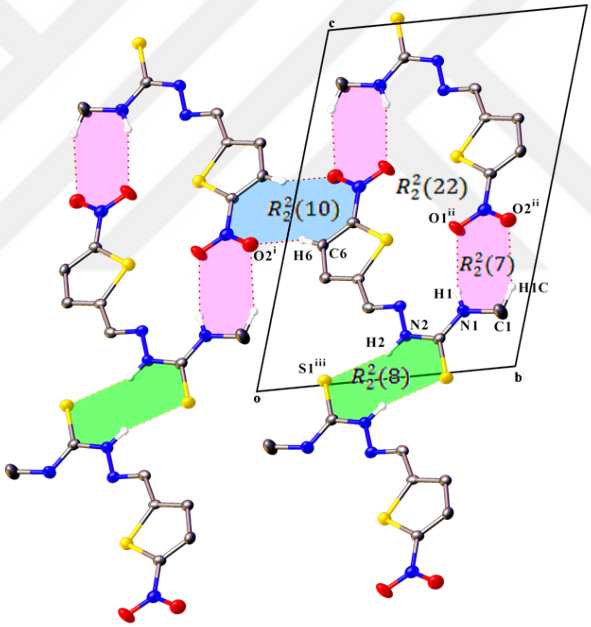

Figure 3.31 Crystal packing of compound TSC[1], showing the formation of a cyclic R rings created by C–H···O, N–H···O and N–H···S hydrogen bonds. H atoms not involved in hydrogen bonding have been omitted for clarity. Symmetry codes are as in Table 3.9

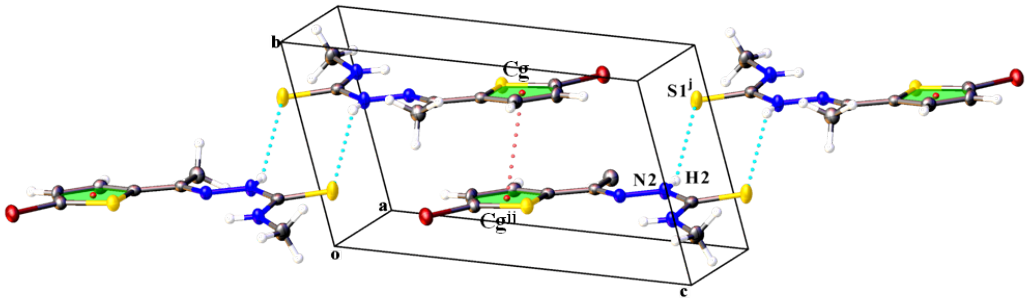

Figure 3.32 Part of the crystal structure of compound TSC[2] showing the formation of hydrogen-bonded dimers running parallel to the (110) plane, and stacking of layers linked by π ···π (thiophene ring) intermolecular interactions. H atoms not involved in hydrogen bonding have been omitted for clarity. Symmetry codes: (j) 2-x,1-y,2-z; (jj) 1-x, 1-y, 1-z.

3.8 Antiproliferative Activity

The MTT assay procedure was applied to evaluate the in vitro cytotoxicity of Ru(II) complexes on human A2780 (primary) and human OVCAR-3 (metastatic) ovarian cancer cell lines. Carboplatin, Oxaliplatin and Paclitaxel were used as comperative reference substances, and were investigated at identical conditions. Both cell lines were treated with different concentrations of TSC ligands (25, 50, 100 µM) and Ru(II) complexes (1, 5, 10, 50 µM) for 24 hours. The IC_{50} rate for Ru(II) complexes and reference substances against A2780 and OVCAR-3 cell lines were shown in Table 3.10.

Based on IC_{50} values, it was noticed that the highest cytotoxic activity on A2780 tumor cells was shown by complex II, the highest cytotoxic activity on OVCAR-3 tumor cells was shown by complex III. This study showed that Ru(II) complexes (I, II, and III) were more cytotoxic on OVCAR-3 cell line than chemotherapeutic agents used as reference substances (Carboplatin, Oxaliplatin and Paclitaxel) in the recent study. The situation was slightly different considering the cytotoxicity experiments on A2780 cell line. I and III complexes were more cytotoxic on A2780 cell line than Paclitaxel and Carboplatin. However, Oxaliplatin showed the highest cytotoxic effect on A2780 cells than all Ru(II) complexes. When the IC_{50} values of the newly synthesized ruthenium(II) complexes obtained from the cytotoxicity experiments on

both cell lines were examined, it was observed that the IC_{50} values of the Ru complexes on the A2780 cell line were lower. This showed that ruthenium complexes were more active on the primary ovarian cancer cell line. MTT results on ovarian cancer cell lines of ruthenium(II) complexes are in accordance with the literature studies (Tsovaltzi et al., 2017). Therefore this study suggested that newly synthesized organo ruthenium(II) complexes have strong cytotoxic effect on primary (A2780) and metastatic (OVCAR-3) ovarian cancer cell lines.

Table 3.10 IC_{50} values of newly synthesized TSC ligands and Ru complexes at micromolar (μM) concentration (ND *:Non Detectable)

IC50 Concentration(μM)

Compound	A2780	OVCAR-3	
Ligands	L1	ND*	ND*
	L2	0,8 ± 0,07	11,6 ± 0,2
	L3	0,3 ± 0,06	27,7 ± 0,4
Ru-complexes	Ⅰ	2,1 ± 0,3	5,5 ± 0,4
	Ⅱ	1,7 ± 0,3	3,7 ± 0,3
	Ⅲ	2,1 ± 0,3	1,1 ± 0,2
Commonly used anticancer durgs	Paclitaxes	3,1 ± 0.09	46 ± 0,2
	Oxliplatin	0,9 ± 0.006	828,4 ± 0,1
	Carboplatin	48,7 ± 0,2	42 ± 0,2

CHAPTER FOUR
CONCLUSIONS

In conclusion, this thesis reports synthesis, spectral and structural characterization of novel Ru(II) TSC compounds synthesised from 5-Nitro-2-carboxyaldehydethiophen-*N*-methyl-thiosemicarbazone, 2-Acetyl-5-bromo-thiophen-*N,N*-dimethyl-thiosemicarbazone and 2-Acetyl-5-bromo-thiophen-*N*-methyl-thiosemicarbazone. Chapter 1 gives information about thiosemicarbazones, ruthenium complexes and their structural properties, bonding and stereochemistry of TSCs. Analytical and spectroscopic techniques used for ligands and compounds were discussed. Chapter two is about the synthesis of TSC ligands and their ruthenium (II) complexes. Synthesized ligands are; 5-nitro-2-carboxyaldehydethiophen-*N*-methyl-thiosemicarbazone (TSC^1), 2-acetyl-5-bromo-thiophen-*N*-methyl-thiosemicarbazone (TSC^2) and 2-acetyl-5-bromo-thiophen-*N,N*-dimethyl-thiosemicarbazone (TSC^3). These ligands are characterized by FT-IR, UV-Vis and ^{1}H NMR techniques. Synthesized complexes are; [(η^6-p-cym)RuCl(*N,S*-TSC^1)]Cl, [(η^6-p-cym)RuCl(*N,S*-TSC^2)]Cl, [(η^6-p-cym)RuCl(*N,S*-TSC^3)]Cl, these complexes are characterized by elemental analysis, ^{1}H NMR spectroscopy, FT-IR, single-crystal XRD and MALDI-TOF mass spectrometry. Biological potency of the ligands (TSC^1, TSC^2 and TSC^3) and their corresponding Ru(II) compounds (I, II and III) were investigated on human primary ovarian (A2780) and human metastatic ovarian (OVCAR-3) cell lines. Chapter 3 presents results and discussion parts.

FT-IR and ^{1}H NMR results of ruthenium complexes showed that all ligands are coordinated to the central metal as a bidentate ligand coordinating *via* azomethine nitrogens (C=N) and sulphur atoms to the central metal in all complexes. [(η^6-p-cym)RuCl(*N,S*-TSC^1)]Cl, [(η^6-p-cym)RuCl(*N,S*-TSC^2)]Cl and [(η^6-p-cym)RuCl(*N,S*-TSC^3)]Cl complexes are coordinated as the thione form

Today, it is known that chemotherapeutic drugs, which are still widely used in cancer treatment, are not fully effective on all types of cancer, they cause drug resistance, and there have many important side effects. These adverse effects have led researchers to focus on metal-based anticancer drugs that show less toxicity and high

selectivity to cancer cells. At this point, studies have rapidly increased in the field of metal based pharmaceuticals in the treatment of cancer cells. Ruthenium complexes, metalopharmaceutical compounds, have shown attracting properties including high ligand exchange rates, higher cytotoxic effects, high selectivity. Within the scope of this study, TSC ligands (TSC^1, TSC^2 and TSC^3) and arene Ru(II) complexes (I, II and III) were synthesized and characterized structurally, and their biological potency were also investigated. It was seen that newly synthesized Ru(II) complexes were found to be taken into cancer cells effectively within 24 hours, and had strong cytotoxic effect on ovarian cancer cell lines. Considering the results of this study, it is thought that the newly synthesized organo Ru(II) complexes (I, II and III) may be potential molecules for effective treatment for the patients who have been diagnosed with ovarian cancer.

Acknowledgments

The authors are grateful to the Dokuz Eylul University Rectorship, Scientific Research Project Coordination Center for the financial support of this work, project number 2017.KB.FEN.041 and 2019.KB.FEN.033. DEU, for the use of the Oxford Rigaku Xcalibur Eos Diffractometer (University Research Grant No: 2010.KB.FEN.13) is greatly acknowledged.

Accession codes

CCDC 2015107 and 2015108 contains the supplementary crystallographic data for the compounds TSC^1 and TSC^2, respectively. These data can be obtained free of charge from The Cambridge Crystallographic Data Centre via www.ccdc.cam.ac.uk/data_request/cif.

REFERENCES

Aird, R. E., Cummings, J., Ritchie, A. A., Muir, M., Morris, R. E., Chen, H., ... & Jodrell, D. I. (2002). In vitro and in vivo activity and cross resistance profiles of novel ruthenium (II) organometallic arene complexes in human ovarian cancer. *British Journal of Cancer*, *86*(10), 1652-1657. https://doi.org/10.1038/sj.bjc.6600290

Ali, I., Wani, W. A., & Saleem, K. (2013). Empirical formulae to molecular structures of metal complexes by molar conductance. *Synthesis and Reactivity in Inorganic, Metal-Organic, and Nano-Metal Chemistry*, *43*(9), 1162-1170. https://doi.org/10.1080/15533174.2012.756898

Aman, F., Hanif, M., Kubanik, M., Ashraf, A., Söhnel, T., Jamieson, S. M., ... & Hartinger, C. G. (2017). Anti-inflammatory Oxicams as multi-donor ligand systems: ph-and solvent-dependent coordination modes of Meloxicam and Piroxicam to Ru and Os. *Chemistry–A European Journal*, *23*(20), 4893-4902. https://doi.org/10.1002/chem.201700263

Ashfield, L. J., Cowley, A. R., Dilworth, J. R., & Donnelly, P. S. (2004). Functionalized thiosemicarbazone clusters of copper (I) and silver (I). *Inorganic Chemistry*, *43*(14), 4121-4123. https://doi.org/10.1021/ic035451+

Babak, M. V., Meier, S. M., Huber, K. V., Reynisson, J., Legin, A. A., Jakupec, M. A., ... & Hartinger, C. G. (2015). Target profiling of an antimetastatic RAPTA agent by chemical proteomics: relevance to the mode of action. *Chemical Science*, *6*(4), 2449-2456. https://doi.org/10.1039/C4SC03905J

Beckford, F. A., Leblanc, G., Thessing, J., Shaloski Jr, M., Frost, B. J., Li, L., & Seeram, N. P. (2009). Organometallic ruthenium complexes with thiosemicarbazone ligands: Synthesis, structure and cytotoxicity of [(η6-p-cymene) Ru (NS) Cl]+(NS= 9-anthraldehyde thiosemicarbazones). *Inorganic Chemistry Communications*, *12*(11), 1094-1098. https://doi.org/10.1016/j.inoche.2009.08.034

Bennett, M. A. (1997). Recent advances in the chemistry of arene complexes of ruthenium (0) and ruthenium (II). *Coordination Chemistry Reviews*, *166*, 225-254. https://doi.org/10.1016/S0010-8545(97)00024-6

Bennett, M. A., & Smith, A. K. (1974). Arene ruthenium (II) complexes formed by dehydrogenation of cyclohexadienes with ruthenium (III) trichloride. *Journal of the Chemical Society, Dalton Transactions*, (2), 233-241. https://doi.org/10.1039/DT9740000233

Bennett, M. A., Huang, T. N., Matheson, T. W., Smith, A. K., Ittel, S., & Nickerson, W. (1982). 16.(η6-Hexamethylbenzene) Ruthenium Complexes. *Inorganic Syntheses*, *21*, 74-78. https://doi.org/10.1002/9780470132524.ch16

Bermejo, E., Carballo, R., Castiñeiras, A., Domínguez, R., Maichle-Mössmer, C., Strähle, J., & West, D. X. (1999). Synthesis, characterization and antifungal activity of group 12 metal complexes of 2-acetylpyridine-4N ethylthiosemicarbazone (H4EL) and 2-acetylpyridine-N-oxide-4N-ethylthiosemicarbazone (H4ELO). *Polyhedron*, *18*(27), 3695-3702. https://doi.org/10.1016/S0277-5387(99)00309-5

Bernstein, J., Davis, R. E., Shimoni, L., & Chang, N. L. (1995). Patterns in hydrogen bonding: functionality and graph set analysis in crystals. *Angewandte Chemie International Edition in English*, *34*(15), 1555-1573. https://doi.org/10.1002/anie.199515551

Blanck, S., Maksimoska, J., Baumeister, J., Harms, K., Marmorstein, R., & Meggers, E. (2012). The art of filling protein pockets efficiently with octahedral metal complexes. *Angewandte Chemie International Edition*, *51*(21), 5244-5246. https://doi.org/10.1002/anie.201108865

Cao, W., Zheng, W., & Chen, T. (2015). Ruthenium polypyridyl complex inhibits growth and metastasis of breast cancer cells by suppressing FAK signaling with enhancement of TRAIL-induced apoptosis. *Scientific Reports*, *5*(1), 1-11. https://doi.org/10.1038/srep09157

Casas, J. S., Castellano, E. E., Ellena, J., García-Tasende, M. S., Sánchez, A., Sordo, J., ... & Vidarte, M. J. (2003). Synthesis, spectroscopic and structural aspects of mono-and diorganothallium (iii) complexes of 2, 6-diacetylpyridine bis (thiosemicarbazone)(H2DAPTSC)—A New Coordination Mode of the HDAPTSC—Anion. *Zeitschrift für Anorganische und Allgemeine Chemie*, *629*(2), 261-267. https://doi.org/10.1002/zaac.200390042

Casini, A., Mastrobuoni, G., Ang, W. H., Gabbiani, C., Pieraccini, G., Moneti, G., ... & Messori, L. (2007). ESI–MS characterisation of protein adducts of anticancer ruthenium (ii)-arene PTA (RAPTA) complexes. *ChemMedChem: Chemistry Enabling Drug Discovery*, *2*(5), 631-635. https://doi.org/10.1002/cmdc.200600258

Ceylan, Ü., Tanak, H., Gümüş, S., & Ağar, E. (2011). 2-Ethyl-N-[(5-nitrothiophen-2-yl) methylidene] aniline. *Acta Crystallographica Section E: Structure Reports Online*, *67*(8), o2004-o2004. https://doi.org/10.1107/S1600536811024615

Cozzi, P. G. (2004). Metal–Salen Schiff base complexes in catalysis: practical aspects. *Chemical Society Reviews*, *33*(7), 410-421. https://doi.org/10.1039/B307853C

Da Silva, C. M., da Silva, D. L., Modolo, L. V., Alves, R. B., de Resende, M. A., Martins, C. V., & de Fátima, Â. (2011). Schiff bases: A short review of their antimicrobial activities. *Journal of Advanced Research*, *2*(1), 1-8. https://doi.org/10.1016/j.jare.2010.05.004

Das, A., Peng, S. M., Lee, G. H., & Bhattacharya, S. (2004). Synthesis, structure and electrochemical properties of a group of ruthenium (III) complexes of N-(aryl) picolinamide. *New Journal of Chemistry*, *28*(6), 712-717. https://doi.org/10.1039/B317018G

Das, S., Sinha, S., Britto, R., Somasundaram, K., & Samuelson, A. G. (2010). Cytotoxicity of half sandwich ruthenium (II) complexes with strong hydrogen bond acceptor ligands and their mechanism of action. *Journal of Inorganic Biochemistry*, *104*(2), 93-104. https://doi.org/10.1016/j.jinorgbio.2009.09.017

Dolomanov, O. V., Bourhis, L. J., Gildea, R. J., Howard, J. A., & Puschmann, H. (2009). OLEX2: a complete structure solution, refinement and analysis program. *Journal of Applied Crystallography*, *42*(2), 339-341. https://doi.org/10.1107/S0021889808042726

Dwyer, F. P., Gyarfas, E. C., Rogers, W. P., & KOCH, J. H. (1952). Biological activity of complex ions. *Nature*, *170*(4318), 190-191. https://doi.org/10.1038/170190a0

El-Behery, M., & El-Twigry, H. (2007). Synthesis, magnetic, spectral, and antimicrobial studies of Cu (II), Ni (II) Co (II), Fe (III), and UO2 (II) complexes of a new Schiff base hydrazone derived from 7-chloro-4-hydrazinoquinoline. *Spectrochimica Acta Part A: Molecular and Biomolecular Spectroscopy*, *66*(1), 28-36. https://doi.org/10.1016/j.saa.2006.02.017

Fanni, S., Murphy, S., Killeen, J. S., & Vos, J. G. (2000). Site-specific methylation of coordinated 1, 2, 4-triazoles: A novel route to sterically hindered Ru (bpy) 2 complexes. *Inorganic Chemistry*, *39*(6), 1320-1321. https://doi.org/10.1021/ic991103p

Frezza, M., Hindo, S., Chen, D., Davenport, A., Schmitt, S., Tomco, D., & Ping Dou, Q. (2010). Novel metals and metal complexes as platforms for cancer therapy. *Current Pharmaceutical Design*, *16*(16), 1813-1825. https://doi.org/10.2174/138161210791209009

Fujita, M., Tominaga, M., Hori, A., & Therrien, B. (2005). Coordination assemblies from a Pd (II)-cornered square complex. *Accounts of Chemical Research*, *38*(4), 369-378. https://doi.org/10.1021/ar040153h

García-Raso, Á., Fiol, J. J., Bádenas, F., & Muñoz, F. (2001). Bioinorganic chemistry of copper (II) complexes of N-salicylidene-aminoacidato: Associative versus dissociative mechanism in the formation of copper ternary complexes with

2-aminopyridine (or pyrimidine). An ab initio study. *Polyhedron*, *20*(20), 2609-2618. https://doi.org/10.1016/S0277-5387(01)00874-9

García-Tojal, J., Pizarro, J. L., García-Orad, A., Pérez-Sanz, A. R., Ugalde, M., Díaz, A. A., ... & Rojo, T. (2001). Biological activity of complexes derived from thiophene-2-carbaldehyde thiosemicarbazone. Crystal structure of [Ni (C6H6N3S2) 2]. *Journal of Inorganic Biochemistry*, *86*(2-3), 627-633. https://doi.org/10.1016/S0162-0134(01)00210-0

Geiger, H. C., Donohoe, J. S., & Geiger, D. K. (2014). 4-Bromo-2-(5-bromothiophen-2-yl)-1-[(5-bromothiophen-2-yl) methyl]-5, 6-dimethyl-1H-benzimidazole. *Acta Crystallographica Section E: Structure Reports Online*, *70*(4), o486-o487. https://doi.org/10.1107/S160053681400628X

Geldbach, T. J., Pregosin, P. S., Albinati, A., & Rominger, F. (2001). Phosphino− arene Ruthenium complexes containing the Phosphorus acid anion {P (O)(OR) 2} as P-Donor. *Organometallics*, *20*(10), 1932-1938. https://doi.org/10.1021/om000954y

Ghebreyessus, K. Y., & Nelson, J. H. (2000). Base-promoted hydroalkylation reactions of 1, 3, 5-Me3C6H3, p-MeC6H4CHMe2, C6Me6, p-MeC6H4Me, and MeC6H5 ligands coordinated to Ruthenium (II). *Organometallics*, *19*(17), 3387-3392. https://doi.org/10.1021/om000375t

Ghosh, B., Adak, P., Naskar, S., Pakhira, B., Mitra, P., & Chattopadhyay, S. K. (2017). Ruthenium (II/III) complexes of redox non-innocent bis (thiosemicarbazone) ligands: Synthesis, X-ray crystal structures, electrochemical,

DNA binding and DFT studies. *Polyhedron*, *131*, 74-85. https://doi.org/10.1016/j.poly.2017.04.013

Gil, M., Bermejo, E., Castiñeiras, A., Beraldo, H., & West, D. X. (2000). Structural and spectral study of Nickel (II) complexes of pyridyl bis {3-piperidyl-, bis {hexamethyleneiminyl-, bis {N (4)-diethyl-, and bis {N (4)-dipropylthiosemicarbazones}. *Zeitschrift für Anorganische und Allgemeine Chemie*, *626*(11), 2353-2360. https://doi.org/10.1002/1521-3749(200011)626:11<2353::AID-ZAAC2353>3.0.CO;2-H

Gill, M. R., & Thomas, J. A. (2012). Ruthenium (II) polypyridyl complexes and DNA—from structural probes to cellular imaging and therapeutics. *Chemical Society Reviews*, *41*(8), 3179-3192. https://doi.org/10.1039/C2CS15299A

Gómez-Saiz, P., García-Tojal, J., Maestro, M. A., Mahía, J., Arnaiz, F. J., Lezama, L., & Rojo, T. (2003). New 1, 3, 4-Oxadiazolecopper (ii) derivatives obtained from thiosemicarbazone complexes. *European Journal of Inorganic Chemistry*, *2003*(14), 2639-2650. https://doi.org/10.1002/ejic.200200689

Guo, Z., Xing, R., Liu, S., Zhong, Z., Ji, X., Wang, L., & Li, P. (2007). Antifungal properties of Schiff bases of chitosan, N-substituted chitosan and quaternized chitosan. *Carbohydrate Research*, *342*(10), 1329-1332. https://doi.org/10.1016/j.carres.2007.04.006

Haas, K. L., & Franz, K. J. (2009). Application of metal coordination chemistry to explore and manipulate cell biology. *Chemical Reviews*, *109*(10), 4921-4960. https://doi.org/10.1021/cr900134a

Halfpenny, J., & Sloman, Z. S. (2000). An effective self-templating ring closure method for mixed donor thiophene-based macrocycles. *Journal of the Chemical Society, Perkin Transactions 1*, (12), 1877-1879. https://doi.org/10.1039/B002029J

Huang, H., Zhang, P., Yu, B., Chen, Y., Wang, J., Ji, L., & Chao, H. (2014). Targeting nucleus DNA with a cyclometalated dipyridophenazineruthenium (II) complex. *Journal of Medicinal Chemistry*, *57*(21), 8971-8983. https://doi.org/10.1021/jm501095r

Jiménez, C. A., & Belmar, J. B. (2005). Synthesis of highly hindered polyanionic chelating ligands. *Tetrahedron*, *61*(16), 3933-3938. https://doi.org/10.1016/j.tet.2005.02.064

Jones, R. D., Summerville, D. A., & Basolo, F. (1979). Synthetic oxygen carriers related to biological systems. *Chemical Reviews*, *79*(2), 139-179.

Jouad, E. M., Riou, A., Allain, M., Khan, M. A., & Bouet, G. M. (2001). Synthesis, structural and spectral studies of 5-methyl 2-furaldehyde thiosemicarbazone and its Co, Ni, Cu and Cd complexes. *Polyhedron*, *20*(1-2), 67-74. https://doi.org/10.1016/S0277-5387(00)00598-2

Kilpin, K. J., & Dyson, P. J. (2013). Enzyme inhibition by metal complexes: concepts, strategies and applications. *Chemical Science*, *4*(4), 1410-1419. https://doi.org/10.1039/C3SC22349C

Komor, A. C., & Barton, J. K. (2013). The path for metal complexes to a DNA target. *Chemical Communications*, *49*(35), 3617-3630. https://doi.org/10.1039/C3CC00177F

Köysal, Y., Bülbül, H., Gümüş, S., Ağar, E., & Soylu, M. S. (2016). Crystal structure and computational study of 2, 4-dichloro-N-[(E)-(5-nitrothiophen-2-yl) methylidene] aniline. *Acta Crystallographica Section E: Crystallographic Communications*, *72*(8), 1187-1189. https://doi.org/10.1107/S2056989016011816

Koziol, A. E., Palenik, R. C., & Palenik, G. J. (1988). Nonbonded interactions. A thiophene S··· N intramolecular attraction. Crystal structure of 2-formylthiophene semicarbazone. *Journal of the Chemical Society, Chemical Communications*, (3), 226-227. https://doi.org/10.1039/C39880000226

Labisbal, E., Haslow, K. D., Sousa-Pedrares, A., Valdés-Martínez, J., Hernández-Ortega, S., & West, D. X. (2003). Copper (II) and nickel (II) complexes of 5-methyl-2-hydroxyacetophenone N (4)-substituted thiosemicarbazones. *Polyhedron*, *22*(20), 2831-2837. https://doi.org/10.1016/S0277-5387(03)00405-4

Lapasam, A., Banothu, V., Addepally, U., & Kollipara, M. R. (2020). Half-sandwich arene ruthenium, rhodium and iridium thiosemicarbazone complexes: synthesis, characterization and biological evaluation. *Journal of Chemical Sciences*, *132*(1), 1-10. https://doi.org/10.1007/s12039-019-1731-5

Latheef, L., Manoj, E., & Prathapachandra Kurup, M. R. (2006). Salicylaldehyde 4, 4′-(hexane-1, 6-diyl) thiosemicarbazone. *Acta Crystallographica Section C: Crystal Structure Communications*, *62*(1), o16-o18. https://doi.org/10.1107/S010827010503564X

Lhuachan, S., Siripaisarnpipat, S., & Chaichit, N. (2003). Synthesis, spectra and crystal structure of two copper (I) complexes of acetonethiosemicarbazone. *European Journal of Inorganic Chemistry*, *2003*(2), 263-267. https://doi.org/10.1002/ejic.200390035

Li, H., & Li, L. (2009). 3, 3′, 5, 5′-Tetrabromo-2, 2′-bithiophene. *Acta Crystallographica Section E: Structure Reports Online*, *65*(5), o952-o952. https://doi.org/10.1107/S1600536809011647

Liang, R., Wei, M., Evans, D. G., & Duan, X. (2014). Inorganic nanomaterials for bioimaging, targeted drug delivery and therapeutics. *Chemical Communications*, *50*(91), 14071-14081. https://doi.org/10.1039/C4CC03118K

Liu, Y., Chen, T., Liu, J., & Wong, Y. S. (2013). Identification of fluorescent ruthenium complexes containing imidazole derivatives as a new class of apoptosis inducers by living cell real-time imaging. *MedChemComm*, *4*(5), 865-869. https://doi.org/10.1039/C3MD20237B

Lobana, T. S., Bawa, G., Butcher, R. J., Liaw, B. J., & Liu, C. W. (2006). Thiosemicarbazonates of ruthenium (II): crystal structures of [bis (diphenylphosphino) butane][bis (pyridine-2-carbaldehydethiosemicarbazonato)] ruthenium (II) and [bis (triphenylphosphine)][bis (benzaldehydethiosemicarbazonato)] ruthenium (II). *Polyhedron*, *25*(15), 2897-2903. https://doi.org/10.1016/j.poly.2006.04.018

Lobana, T. S., Khanna, S., & Butcher, R. J. (2007). The influence of the methyl substituents at c2 carbon of thiosemicarbazones {R1R2C2= N3-N2H-C1 (= S)

N1H2} on bonding and structures of copper (I) complexes. *Zeitschrift für Anorganische und Allgemeine Chemie*, *633*(11-12), 1820-1826. https://doi.org/10.1002/zaac.200700199

Lobana, T. S., Khanna, S., Butcher, R. J., Hunter, A. D., & Zeller, M. (2007). Methyl substituent at c2 carbon of acetophenone thiosemicarbazone induces unusual heterobridging in the [(Ph3P) Cu (μ-I) 2 (μ-S-Haptsc) Cu (PPh3)] Dimer. *Inorganic Chemistry*, *46*(15), 5826-5828. https://doi.org/10.1021/ic700401h

Lobana, T. S., Kumari, P., & Butcher, R. J. (2008). Cyclopentanone thiosemicarbazone (Hcptsc) induces a new bonding pattern in (Ph3P) Cu (μ-Br)(μ3-S, N–Hcptsc) CuBr (PPh3) dimer. *Inorganic Chemistry Communications*, *11*(1), 11-14. https://doi.org/10.1016/j.inoche.2007.10.001

Lobana, T. S., Rekha,†, Butcher, R. J., Castineiras, A., Bermejo, E., & Bharatam, P. V. (2006). Bonding trends of thiosemicarbazones in mononuclear and dinuclear copper (I) complexes: syntheses, structures, and theoretical aspects. *Inorganic Chemistry*, *45*(4), 1535-1542. https://doi.org/10.1021/ic051018j

Lobana, T. S., Sharma, R., Bawa, G., & Khanna, S. (2009). Bonding and structure trends of thiosemicarbazone derivatives of metals—an overview. *Coordination Chemistry Reviews*, *253*(7-8), 977-1055. https://doi.org/10.1016/j.ccr.2008.07.004

Manimaran, A., & Jayabalakrishnan, C. (2012). DNA-binding, catalytic oxidation, CC coupling reactions and antibacterial activities of binuclear Ru (II) thiosemicarbazone complexes: Synthesis and spectral characterization. *Journal of Advanced Research*, *3*(3), 233-243. https://doi.org/10.1016/j.jare.2011.07.005

Manivannan, S., Prabhakaran, R., Balasubramanian, K. P., Dhanabal, V., Karvembu, R., Chinnusamy, V., & Natarajan, K. (2007). Synthesis, spectral, electrochemical and catalytic studies of new Ru (III) tetradentate Schiff base complexes. *Applied Organometallic Chemistry*, *21*(11), 952-957. https://doi.org/10.1002/aoc.1318

Maurya, R. C., Pandey, A., Chaurasia, J., & Martin, H. (2006). Metal nitrosyl complexes of bioinorganic, catalytic, and environmental relevance: a novel single-step synthesis of dinitrosylmolybdenum (0) complexes of {Mo (NO) 2} 6 electron configuration involving Schiff bases derived from 4-acyl-3-methyl-1-phenyl-2-pyrazolin-5-one and 4-aminoantipyrine, directly from molybdate (VI) and their characterization. *Journal of Molecular Structure*, *798*(1-3), 89-101. https://doi.org/10.1016/j.molstruc.2006.03.094

McBurney, B., Crundwell, G., Updegraff III, J. B., Zeller, M., & Hunter, A. D. (2005). 5-Nitrothiophene-2-carbaldehyde. *Acta Crystallographica Section E: Structure Reports Online*, *61*(5), o1221-o1222. https://doi.org/10.1107/S1600536805009979

Meggers, E. (2007). Exploring biologically relevant chemical space with metal complexes. *Current Opinion in Chemical Biology*, *11*(3), 287-292. https://doi.org/10.1016/j.cbpa.2007.05.013

Meggers, E. (2009). Targeting proteins with metal complexes. *Chemical Communications*, (9), 1001-1010. https://doi.org/10.1039/B813568A

Miroslaw, B., Szulczyk, D., Koziol, A. E., & Struga, M. (2011). 4-(3-Fluorophenyl)-1-(propan-2-ylidene) thiosemicarbazone. *Acta Crystallographica Section E:*

Structure Reports Online, *67*(11), o3010-o3010. https://doi.org/10.1107/S1600536811042504

Morris, G. A., Zhou, H., Stern, C. L., & Nguyen, S. T. (2001). A general high-yield route to bis (salicylaldimine) zinc (II) complexes: Application to the synthesis of pyridine-modified salen-type zinc (II) complexes. *Inorganic Chemistry*, *40*(13), 3222-3227. https://doi.org/10.1021/ic010090o

Muetterties, E. L., Bleeke, J. R., & Sievert, A. C. (1979). Arene transition metal chemistry: III. Arene exchange phenomena. *Journal of Organometallic Chemistry*, *178*(1), 197-216. https://doi.org/10.1016/S0022-328X(00)87871-7

Nehar, O., Louhibi, S., Boukli-Hacene, L., & Roisnel, T. (2016). Synthesis and crystal structure of ((E)-{2-[(E)-(4-hydroxynaphthalen-1-yl) methylidene] hydrazin-1-yl}(methylsulfanyl) methylidene) azanium hydrogen sulfate monohydrate. *Acta Crystallographica Section E: Crystallographic Communications*, *72*(9), 1326-1329. https://doi.org/10.1107/S2056989016013232

Olive, G. H., & Olive, S. (1984). The chemistry of the Catalyzed Hydrogenation of Carbon Monoxide. *Berlin: Springer*, *152*(1), 301-315.

Pal, I., Basuli, F., Mak, T. C., & Bhattacharya, S. (2001). Synthesis, structure, and properties of a novel heterooctametallic complex containing a cyclic RU4Ni4 core. *Angewandte Chemie*, *113*(15), 3007-3009. https://doi.org/10.1002/1521-3757(20010803)113:15<3007::AID-ANGE3007>3.0.CO;2-I

Pappenfus, T. M., Wood, T. L., Morey, J. L., Wilcox, W. D., & Janzen, D. E. (2018). Crystal structure and hirshfeld analysis of 2-(5-bromothiophen-2-yl) acetonitrile.

Acta Crystallographica Section E: Crystallographic Communications, *74*(2), 189-192. https://doi.org/10.1107/S2056989018000968

Parsons, S., Smith, A. G., Tasker, P. A., & White, D. J. (2000). Acetone-4-methylthiosemicarbazone at 220 K. *Acta Crystallographica Section C: Crystal Structure Communications*, *56*(2), 237-238. https://doi.org/10.1107/S0108270199014559

Pascu, G. I., Hotze, A. C., Sanchez-Cano, C., Kariuki, B. M., & Hannon, M. J. (2007). Dinuclear ruthenium (II) triple-stranded helicates: luminescent supramolecular cylinders that bind and coil DNA and exhibit activity against cancer cell lines. *Angewandte Chemie International Edition*, *46*(23), 4374-4378. https://doi.org/10.1002/anie.200700656

Pattan, S. R., Pawar, S. B., Vetal, S. S., Gharate, U. D., & Bhawar, S. B. (2012). The scope of metal complexes in drug design-a review. *Indian Drugs*, *49*(11), 5-12.

Pedrido, R., Bermejo, M. R., Romero, M. J., Vázquez, M., González-Noya, A. M., Maneiro, M., ... & Fernández, M. I. (2005). Syntheses and X-ray characterization of metal complexes with the pentadentate thiosemicarbazone ligand bis (4-N-methylthiosemicarbazone)-2, 6-diacetylpyridine. The first pentacoordinate lead (II) complex with a pentagonal geometry. *Dalton Transactions*, (3), 572-579. https://doi.org/10.1039/B416296J

Przybylski, P., Huczynski, A., Pyta, K., Brzezinski, B., & Bartl, F. (2009). Biological properties of Schiff bases and azo derivatives of phenols. *Current Organic Chemistry*, *13*(2), 124-148. https://doi.org/10.2174/138527209787193774

Puckett, C. A., & Barton, J. K. (2007). Methods to explore cellular uptake of ruthenium complexes. *Journal of the American Chemical Society*, *129*(1), 46-47. https://doi.org/10.1021/ja0677564

Puckett, C. A., Ernst, R. J., & Barton, J. K. (2010). Exploring the cellular accumulation of metal complexes. *Dalton Transactions*, *39*(5), 1159-1170. https://doi.org/10.1039/B922209J

Qian, C., Wang, J. Q., Song, C. L., Wang, L. L., Ji, L. N., & Chao, H. (2013). The induction of mitochondria-mediated apoptosis in cancer cells by ruthenium (II) asymmetric complexes. *Metallomics*, *5*(7), 844-854. https://doi.org/10.1039/c3mt20270d

Raja, M. U., Sindhuja, E., & Ramesh, R. (2010). Arene ruthenium (II) p-chloroacetophenone phenylthiosemicarbazone complex mediated transfer hydrogenation of ketones. *Inorganic Chemistry Communications*, *13*(11), 1321-1324. https://doi.org/10.1016/j.inoche.2010.07.026

Robertson, D. R., & Stephenson, T. A. (1976). Reaction of [η6-C6H6 RuCl2] 2 and [η5-C5Me5RhCl2] 2 with some sulphur-containing nucleophiles. *Journal of Organometallic Chemistry*, *107*(3), C46-C48. https://doi.org/10.1016/S0022-328X(00)91534-1

Sakthivel, A., Jeyasubramanian, K., Thangagiri, B., & Raja, J. D. (2020). Recent advances in Schiff base metal complexes derived from 4-aminoantipyrine derivatives and their potential applications. *Journal of Molecular Structure*, *1222*, 128885. https://doi.org/10.1016/j.molstruc.2020.128885

Salga, M. S., Ali, H. M., Abdulla, M. A., & Abdelwahab, S. I. (2012). Acute oral toxicity evaluations of some zinc (II) complexes derived from 1-(2-Salicylaldiminoethyl) piperazine schiff bases in rats. *International Journal of Molecular Sciences*, *13*(2), 1393-1404. https://doi.org/10.3390/ijms13021393

Sawodny, W., & Riederer, M. (1977). Addition compounds with polymeric chromium (ii)-schiff base complexes. *Angewandte Chemie International Edition in English*, *16*(12), 859-860.

Sharma, R. K., Singh, R. V., & Tandon, J. P. (1980). Biscyclopentadienyl titanium (IV) complexes of monofunctional bidentate ketamines. *Journal of Inorganic and Nuclear Chemistry*, *42*(9), 1382-1384. https://doi.org/10.1016/0022-1902(80)80313-7

Sheldrick, G. M. (2015). Crystal structure refinement with SHELXL. *Acta Crystallographica Section C: Structural Chemistry*, *71*(1), 3-8. https://doi.org/10.1107/S2053229614024218

Shimakoshi, H., Goto, A., Tachi, Y., Naruta, Y., & Hisaeda, Y. (2001). Synthesis and redox behavior of dialkylated dicobalt complexes having two discrete salen units. *Tetrahedron Letters*, *42*(10), 1949-1951. https://doi.org/10.1016/S0040-4039(01)00040-5

Siddiqui, E. J., Azad, I., Khan, A. R., & Khan, T. (2019). Thiosemicarbazone complexes as versatile medicinal chemistry agents: a review. *Journal of Drug Delivery and Therapeutics*, *9*(3), 689-703. https://doi.org/10.22270/jddt.v9i3.2888

Sivagamasundari, M., & Ramesh, R. (2007). Luminescent property and catalytic activity of Ru (II) carbonyl complexes containing N, O donor of 2-hydroxy-1-naphthylideneimines. *Spectrochimica Acta Part A: Molecular and Biomolecular Spectroscopy*, *66*(2), 427-433. https://doi.org/10.1016/j.saa.2006.03.017

Souza, A. O. D., Galetti, F., Silva, C. L., Bicalho, B., Parma, M. M., Fonseca, S. F., ... & De Oliveira, M. C. (2007). Antimycobacterial and cytotoxicity activity of synthetic and natural compounds. *Química Nova*, *30*, 1563-1566. https://doi.org/10.1590/S0100-40422007000700012

Spek, A. L. J. (2003). Single-crystal structure validation with the program PLATON. *Journal of Applied Crystallography*, *36*(1), 7-13. https://doi.org/10.1107/S0021889802022112

Stringer, T., Therrien, B., Hendricks, D. T., Guzgay, H., & Smith, G. S. (2011). Mono-and dinuclear (η6-arene) ruthenium (II) benzaldehyde thiosemicarbazone complexes: Synthesis, characterization and cytotoxicity. *Inorganic Chemistry Communications*, *14*(6), 956-960. https://doi.org/10.1016/j.inoche.2011.03.041

Su, W., Zhou, Q., Huang, Y., Huang, Q., Huo, L., Xiao, Q., ... & Li, P. (2013). Synthesis, crystal and electronic structure, anticancer activity of ruthenium (II) arene complexes with thiosemicarbazones. *Applied Organometallic Chemistry*, *27*(5), 307-312. https://doi.org/10.1002/aoc.2977

Subasi, E., Atalay, E. B., Erdogan, D., Sen, B., Pakyapan, B., & Kayali, H. A. (2020). Synthesis and characterization of thiosemicarbazone-functionalized organoruthenium (II)-arene complexes: Investigation of antitumor characteristics

in colorectal cancer cell lines. *Materials Science & Engineering. C, Materials for Biological Applications*, *106*, 110152. https://doi.org/10.1016/j.msec.2019.110152

Tan, C. P., Lu, Y. Y., Ji, L. N., & Mao, Z. W. (2014). Metallomics insights into the programmed cell death induced by metal-based anticancer compounds. *Metallomics*, *6*(5), 978-995. https://doi.org/10.1039/c3mt00225j

Therrien, B. (2009). Functionalised η6-arene ruthenium complexes. *Coordination Chemistry Reviews*, *253*(3-4), 493-519. https://doi.org/10.1016/j.ccr.2008.04.014

Trinajstić, N. (1968). Calculation of carbon-sulphur bond lengths. *Tetrahedron Letters*, *9*(12), 1529-1532.

Tsovaltzi, E., Malamidou-Xenikaki, E., Dalezis, P., Hatzidimitriou, A., Lazarides, T., Trafalis, D., & Sarli, V. (2017). Synthesis and analysis of the anticancer activity of Ru (ii) complexes incorporating 2-hydroxymethylidene-indene-1, 3-dione ligands. *New Journal of Chemistry*, *41*(18), 10438-10446. https://doi.org/10.1039/C7NJ02162C

Turro, C. (2011). To intercalate or semiintercalate, or both?. *Proceedings of the National Academy of Sciences*, *108*(43), 17573-17574. https://doi.org/10.1073/pnas.1114519108

Wang, J. Q., Zhang, P. Y., Qian, C., Hou, X. J., Ji, L. N., & Chao, H. (2014). Mitochondria are the primary target in the induction of apoptosis by chiral ruthenium (II) polypyridyl complexes in cancer cells. *JBIC Journal of Biological Inorganic Chemistry*, *19*(3), 335-348. https://doi.org/10.1007/s00775-013-1069-2

Winkhaus, G., & Singer, H. (1967). Ruthen (II)-komplexe mit zweizähnigem cycloheptatrien und benzol. *Journal of Organometallic Chemistry*, *7*(3), 487-491. https://doi.org/10.1016/S0022-328X(00)85370-X

Wu, K., Hu, W., Luo, Q., Li, X., Xiong, S., Sadler, P. J., & Wang, F. (2013). Competitive binding sites of a ruthenium arene anticancer complex on oligonucleotides studied by mass spectrometry: Ladder-sequencing versus top-down. *Journal of The American Society for Mass Spectrometry*, *24*(3), 410-420. https://doi.org/10.1007/s13361-012-0539-z

Yaman, P. K., Şen, B., Karagöz, C. S., & Subaşı, E. (2017). Half-sandwich ruthenium-arene complexes with thiophen containing thiosemicarbazones: Synthesis and structural characterization. *Journal of Organometallic Chemistry*, *832*, 27-35. https://doi.org/10.1016/j.jorganchem.2017.01.013

Yan, Y. K., Melchart, M., Habtemariam, A., & Sadler, P. J. (2005). Organometallic chemistry, biology and medicine: ruthenium arene anticancer complexes. *Chemical Communications*, (38), 4764-4776. https://doi.org/10.1039/B508531B

Zelonka, R. A., & Baird, M. (1972). Benzene complexes of ruthenium (II). *Canadian Journal of Chemistry*, *50*(18), 3063-3072. https://doi.org/10.1139/v72-486@cjc-csc.issue01

Zeng, L., Gupta, P., Chen, Y., Wang, E., Ji, L., Chao, H., & Chen, Z. S. (2017). The development of anticancer ruthenium (II) complexes: from single molecule compounds to nanomaterials. *Chemical Society Reviews*, *46*(19), 5771-5804.

Zeng, L., Xiao, Y., Liu, J., & Tan, L. (2012). Synthesis, characterization, DNA-binding and cytotoxic properties of Ru (II) complexes:[Ru (MeIm) 4L] 2+(MeIm= 1-methylimidazole, L= phen, ip and pip). *Journal of Molecular Structure*, *1019*, 183-190. https://doi.org/10.1016/j.molstruc.2012.03.023

Zhang, J., Wu, L. P., Zhuang, L. H., & Wang, G. W. (2009). 3-Methoxybenzaldehyde thiosemicarbazone. *Acta Crystallographica Section E: Structure Reports Online*, *65*(4), o884-o884. https://doi.org/10.1107/S160053680901040X

Zhang, L., Carroll, P., & Meggers, E. (2004). Ruthenium complexes as protein kinase inhibitors. *Organic Letters*, *6*(4), 521-523. https://doi.org/10.1021/ol036283s

Zhao, R., Hammitt, R., Thummel, R. P., Liu, Y., Turro, C., & Snapka, R. M. (2009). Nuclear targets of photodynamic tridentate ruthenium complexes. *Dalton Transactions*, (48), 10926-10931. https://doi.org/10.1039/B913959A

Zheng, K., Wu, Q., Wang, C., Tan, W., & Mei, W. (2017). Ruthenium (II) complexes as potential apoptosis inducers in chemotherapy. *Anti-Cancer Agents in Medicinal Chemistry (Formerly Current Medicinal Chemistry-Anti-Cancer Agents)*, *17*(1), 29-39. https://doi.org/10.2174/1871520616666160622085441

Zhou, Y., Yu, Q., Qin, X., Bhavsar, D., Yang, L., Chen, Q., ... & Liu, J. (2016). Improving the anticancer efficacy of laminin receptor-specific therapeutic ruthenium nanoparticles (RuBB-loaded EGCG-RuNPs) via ROS-dependent apoptosis in SMMC-7721 cells. *ACS Applied Materials & Interfaces*, *8*(24), 15000-15012. https://doi.org/10.1021/acsami.5b02261